Supplementary Information

Non-Hydrogen-Bonding-Based, Solvent-Dependent Helix Inversion Between Pure P-Helix and Pure M-Helix in Poly(quinoxaline-2,3-diyl)s Bearing Chiral Side Chains

Tetsuya Yamada,[a] Yuuya Nagata,[a] and Michinori Suginome *[ab]

[a]*Department of Synthetic Chemistry and Biological Chemistry, Graduate School of Engineering, Kyoto University, Katsura, Nishikyo-ku, Kyoto 615-8510, Japan*
[b] *JST, CREST (Creation of Next-Generation Nanosystems through Process Integration), Sanbancho, Chiyodaku, Tokyo, 102-0075, Japan*

Contents

1. General

All reactions were carried out under an atmosphere of nitrogen with magnetic stirring. ^{1}H and ^{13}C NMR spectra were recorded on a Varian Mercury vx400 or a JEOL JNM-A500 spectrometer at ambient temperature. ^{1}H NMR data are reported as follows: chemical shift in ppm downfield from tetramethylsilane (δ scale), multiplicity (s = singlet, d = doublet, t = triplet, q = quartet, quint = quintet, sex = sextet, m = multiplet, and br = broad), coupling constant (Hz), and integration. ^{13}C NMR chemical shifts are reported in ppm downfield from tetramethylsilane (δ scale). All ^{13}C NMR spectra were obtained with complete proton decoupling. CD spectra were recorded on a JASCO J-750 spectrometer. UV spectra were recorded on a JASCO V-500 spectrometer. The GPC analysis was carried out with TSKgel G4000H$_{HR}$ ($CHCl_3$, polystyrene standard). Preparative GPC was performed on JAI LC-908 equipped with JAIGEL-1H and -2H columns in a series ($CHCl_3$).

THF was dried and deoxygenized using an alumina/catalyst column system (GlassContour Co.). Trimethylphenylphosphine (Aldrich) and sodium borohydride (Aldrich) were used as received from the commercial sources. Achiral monomer **1** and chiral monomers (*R*)- and (*S*)-**2** and achiral nickel initiator were prepared according to the reported procedures.

2. Experimental Procedures

Synthesis of Monomer (*R*)-2

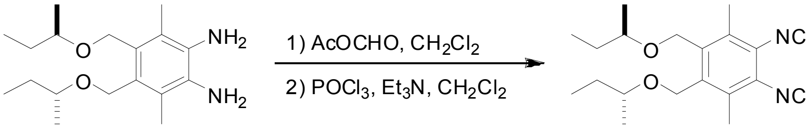

(*R*)-**S1**

(*R*)-**2**

To a CH_2Cl_2 (25 mL) solution of 1,2-amino-3,6-dimethyl-4,5-bis((*R*)-2-butoxymethyl)benzene ((*R*)-**S1**, 1.64 g, 5.32 mmol) was added acetylformate (1.5 mL, 21 mmol) at 0°C . The mixture was stirred for 15 h with gradual warming up to rt. The mixture containing 1,2-diformamido-3,6-dimethyl-4,5-bis((*R*)-2-butoxymethyl)benzene was subjected to evaporation of volatile materials in vacuo and used for the next step without further purification. To a CH_2Cl_2 (50 mL) suspension of the diformamide and Et_3N (7.8 mL, 55 mmol) cooled to 0°C, $POCl_3$ (1.6 mL, 17 mmol) was added. After stirring for 1 h at 0°C, saturated $NaHCO_3$ aq. was added to the reaction mixture. Extraction with CH_2Cl_2 followed by column chromatography on silica gel (hexane:ether = 5:1) gave **(*R*)-2** as white solid (1.00 g, 57% yield).

Typical Procedures for the Synthesis of Poly(quinoxaline-2,3-diyl)s

Synthesis of copolymer poly-1/(*R*)-2(20/20): A THF solution of *o*-TolNiCl(PMe_3)$_2$ (0.050 M, 50 μL, 2.5 μmol) was diluted with THF (3.85 mL). To the solution was added a solution of PMe_3 in THF (1.0 M, 2.5 *μ*L, 2.5 *μ*mol). After stirring for 15 minutes, a solution of monomer **1** (15.0 mg, 50 *μ*mol) and (*R*)-**2** (16.4 mg, 50 *μ*mol) in THF (1.25 mL) was added at room temperature. After 3 h, a THF solution of *o*-TolMgBr (1.0M, 50 μL, 50 *μ*mol) was added to the reaction mixture at room temperature. After stirring for 15 min. at room temperature, water was added. Extraction with $CHCl_3$ followed by preparative GPC gave **poly-1/(*R*)-2(20/20)** as orange solid (29 mg, 92% yield).

Synthesis of homopolymer poly-(*R*)-2: A THF solution of *o*-TolNiCl(PMe_3)$_2$ (0.050 M, 50 *μ*L, 2.5 *μ*mol) was diluted with THF (3.85 mL). To the solution was added a solution of

PMe_3 in THF (1.0 M, 2.5 *μ*L, 2.5 *μ*mol). After stirring for 15 minutes, a solution of (*R*)-**2** (32.8 mg, 100 *μ*mol) in THF (1.25 mL) was added at room temperature. After 3 h, a THF solution of *o*-TolMgBr (1.0M, 50 *μ*L, 50 *μ*mol) was added to the reaction mixture at room temperature. After stirring for 15 min. at room temperature, water was added. Extraction with $CHCl_3$ followed by preparative GPC gave **poly-(*R*)-2** as orange solid (31 mg, 95% yield).

Synthesis of homopolymer poly-(*R*)-2(100): A THF solution of *o*-TolNiCl$(PMe_3)_2$ (0.050 M, 20 *μ*L, 1.0 *μ*mol) was diluted with THF (3.85 mL). To the solution was added a solution of PMe_3 in THF (1.0 M, 2.5 *μ*L, 2.5 *μ*mol). After stirring for 15 minutes, a solution of (*R*)-**2** (32.8 mg, 100 *μ*mol) in THF (1.25 mL) was added at room temperature. After 3 h, a THF solution of *o*-TolMgBr (1.0M, 50 *μ*L, 50 *μ*mol) was added to the reaction mixture at room temperature. After stirring for 15 minutes at room temperature, water was added. Extraction with $CHCl_3$ followed by preparative GPC gave **poly-(*R*)-2(100)** as orange solid (29 mg, 95% yield).

Synthesis of homopolymer poly-(*R*)-2(200): A THF solution of *o*-TolNiCl$(PMe_3)_2$ (0.050 M, 10 *μ*L, 0.50 *μ*mol) was diluted with THF (3.85 mL). To the solution was added a solution of PMe_3 in THF (1.0 M, 2.5 *μ*L, 2.5 *μ*mol). After stirring for 15 min., a solution of (*R*)-**2** (32.8 mg, 100 *μ*mol) in THF (1.25 mL) was added at room temperature. After 3 h, a THF solution of *o*-TolMgBr (1.0 M, 50 *μ*L, 50 *μ*mol) was added to the reaction mixture at room temperature. After stirring for 15 min. at room temperature, water was added. Extraction with $CHCl_3$ followed by preparative GPC gave **poly-(*R*)-2** as orange solid (27 mg, 95% yield).

Procedure for the CD measurements in 1,1,2-TCE/$CHCl_3$ Solution (Figure 2)

Mixed solvents for the CD measurements were prepared by mixing $CHCl_3$ and 1,1,2-TCE by volume. The volume was measured with measuring cylinder.

poly-(*R*)-2 (1.98 mg) was dissolved in $CHCl_3$ in 10 mL measuring flask. A 1 mL portion of the solution was transferred into other 10 mL measuring flasks by use of measuring pipette (1 mL). Chloroform in these flasks were evaporated in vacuo 3 h at room temperature. Each flask containing dried **poly-(*R*)-2** (0.198 mg) was filled with the mixed solvent. After leaving the solution at room temperature for 3 h, the solutions were subjected to CD and UV/Vis measurements.

3. Analytical and NMR Data for New Compounds

Monomer (*R*)- and (*S*)-2

(*R*)-**2**: ^{1}H NMR (400 MHz, $CDCl_3$) δ 0.93 (t, 7.6Hz, 6H), 1.24 (d, 6.4Hz, 6H), 1.45-1.65 (m, 4H), 2.49 (s, 6H), 3.49 (sex, 6.0 Hz, 2H), 4.44 (d, 10.4 Hz, 2H), 4.59 (d, 10.4 Hz, 2H); ^{13}C NMR (125 MHz, $CDCl_3$) δ 9.9, 15.5, 19.1, 29.2, 64.0, 77.7, 123.9, 134.1, 138.3, 172.8; IR (KBr) 2122 cm^{-1}; Anal. Calcd. for $C_{20}H_{28}N_2O_2$: C, 73.14; H, 8.59: N, 8.53. Found: C, 73.29; H, 8.75; N, 8.57**;** $[\alpha]_D$ -29.6 ($CHCl_3$, c = 0.49).

(*S*)-**2;** $[\alpha]_D$ +29.0 ($CHCl_3$, c = 0.49).

Monomer (*S*)-3

(*S*)-**3**: ^{1}H NMR (400 MHz, $CDCl_3$) δ 0.91 (t, 7.2Hz, 6H), 0.99 (d, 6.4Hz, 6H), 1.18-1.50 (m, 10H), 2.39 (s, 6H), 2.55 (dt, 4.8Hz, 12.8Hz, 2H), 2.65 (dt, 4.8Hz, 12.8Hz, 2H); ^{13}C NMR (125 MHz, $CDCl_3$) δ 11.4, 15.7, 19.0, 27.9, 29.2, 35.3, 36.6, 122.0, 131.6, 142.0, 171.4; IR (neat) 2116 cm^{-1}; HRMS Calcd. For $C_{22}H_{32}N_2$: 324.2565. Found 324.2566.**;** $[\alpha]_D$ +11.6 ($CHCl_3$, *c* = 0.50).

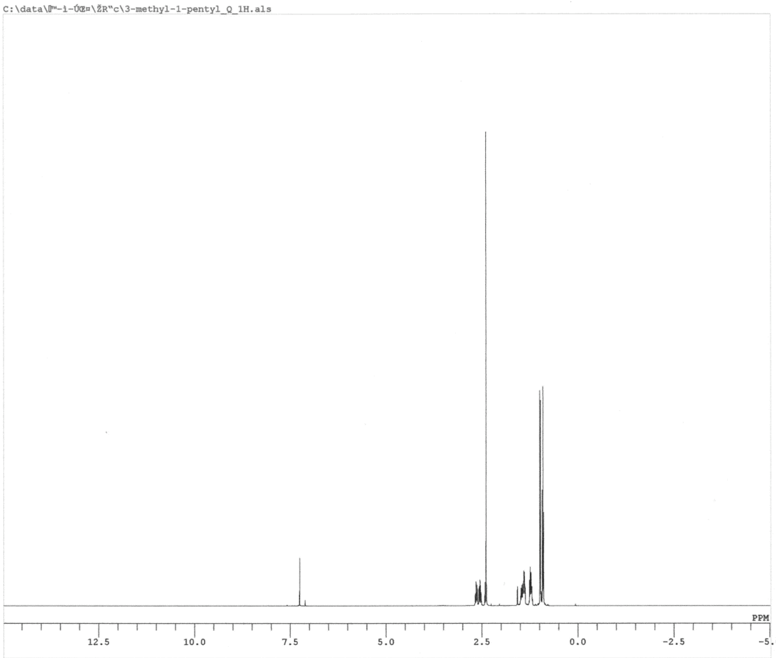

```
EXMOD  SINGL
IRMOD  NON
OBNUC  1H
OBFRQ        500.00 MHz
OBSET          0.00 KHz
PW1            5.50 usec
POINT         32768
SAMPO         32768
TIMES             8
SCANS             8
DUMMY             2
FREQU      10000.00 Hz
FILTR          6000 Hz
ACQTM        3.2768 sec
DEADT         10.00 usec
DELAY         44.64 usec
PD           2.2232 sec
ADBIT            16
RGAIN            16
IRNUC  1H
IRFRQ        500.00 MHz
IRSET          0.00 KHz
IRRPW            40 usec
IRATN           511
IRRNS             0
IRBP1            10
IRBP2             2
BF             0.16 Hz
T1             0.00
T2             0.00
T3            90.00
T4           100.00
XE         10000.00 Hz
XS             0.00 Hz
REFVL
DFILE  3-methyl-1-pentyl_Q_1
MENUF  ogoshih
SHMFL  th5
LKSET          0.00 KHz
LKLEV           200
LGAIN            18
LKPHS           231
LKSIG           805
CTEMP          19.5 c
CSPED            10 Hz
FIELD         -8077
```

^{1}H NMR of (*S*)-3

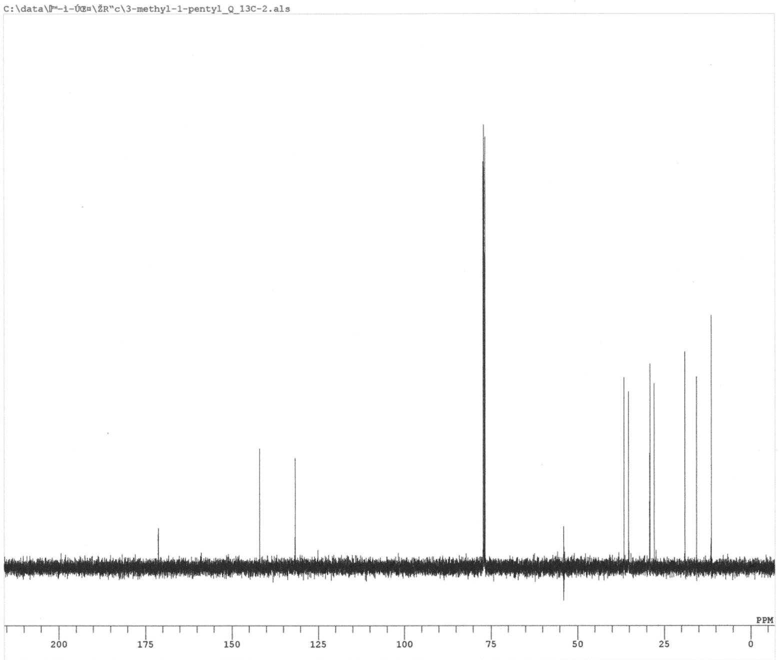

```
EXMOD  SINGL
IRMOD  BCM
OBNUC  13C
OBFRQ        125.65 MHz
OBSET          0.00 KHz
PW1            4.50 usec
POINT         32768
SAMPO         32768
TIMES         29600
SCANS            92
DUMMY            16
FREQU      28011.20 Hz
FILTR         14000 Hz
ACQTM        1.1698 sec
DEADT         19.18 usec
DELAY         14.29 usec
PD           2.0000 sec
ADBIT            16
RGAIN            35
IRNUC  1H
IRFRQ        500.00 MHz
IRSET          0.00 KHz
IRRPW            40 usec
IRATN           511
IRRNS             0
IRBP1            30
IRBP2             6
BF             0.49 Hz
T1             0.00
T2             0.00
T3            90.00
T4           100.00
XE         28011.20 Hz
XS             0.00 Hz
REFVL
DFILE  3-methyl-1-pentyl_Q_1
MENUF  yamada13C
SHMFL  th5
LKSET          0.00 KHz
LKLEV           200
LGAIN            18
LKPHS           231
LKSIG           785
CTEMP          19.9 c
CSPED            11 Hz
FIELD         -8077
```

^{13}C NMR of (*S*)-3

Properties of Homopolymers (poly-1, poly-(*R*)-2 and poly-(*S*)-2) and Random Copolymers (poly-1/(*R*)-2 and poly-1/(*S*)-2)

Table S1. Properties of Homopolymers (poly-**1** and poly-(*R*)-**2**) and Random Copolymers poly-1/(*R*)-**2**

polymer	yield(%)	*M*n/10^4	M_w/M_n	$g_{abs}^{366}/10^{-3}$ (CHCl$_3$)	$g_{abs}^{366}/10^{-3}$ (1,1,2-TCE)
poly-**1**	86	6.8	1.08	-	-
poly-**1**/**2**(95/5)	88	7.5	1.07	0.56	-0.39
poly-**1**/**2**(90/10)	91	7.7	1.07	1.07	-0.67
poly-**1**/**2**(80/20)	87	7.7	1.08	1.76	-1.49
poly-**1**/**2**(70/30)	93	8.2	1.08	2.13	-1.81
poly-**1**/**2**(50/50)	92	7.9	1.08	2.38	-2.49
poly-**1**/**2**(30/70)	88	7.9	1.09	2.34	-2.78
poly-**2**	95	7.9	1.07	2.36	-2.81
poly-**2**(100)	87	28	1.06	2.47	-[a]
poly-**2**(200)	83	58	1.04	2.51	-[a]

a) not determined due to the poor solubility.

Table S2. Properties of Homopolymer poly-(*S*)-**2** and Random Copolymers poly-1/(*S*)-**2**

polymer	yield(%)	*M*n/10^4	M_w/M_n	$g_{abs}^{366}/10^{-3}$(CHCl3)	$g_{abs}^{366}/10^{-3}$ (1,1,2-TCE)
poly-**1**/**2**(90/10)	94	6.8	1.08	-1.03	0.71
poly-**1**/**2**(80/20)	91	7.5	1.07	-1.82	1.59
poly-**1**/**2**(70/30)	89	7.7	1.07	-2.14	2.13
poly-**1**/**2**(50/50)	86	7.7	1.08	-2.34	2.50
poly-**2**	91	8.2	1.08	-2.45	2.83

Table S3. Properties of Homopolymer poly-(*S*)-**3**

polymer	yield(%)	*M*n/10^4	M_w/M_n	$g_{abs}^{366}/10^{-3}$(CHCl3)	$g_{abs}^{366}/10^{-3}$ (1,1,2-TCE)
poly-(*S*)-**3**	88	5.6	1.17	-0.32	1.06

Homopolymer **poly-1**: ^{1}H NMR (400MHz, CDCl$_3$) δ 0.88 (brs, 6*n*H), 1.59 (brs, 4*n*H), 2.34 (brs, 6*n*H), 3.46 (brs, 4*n*H), 4.58 (brs, 2*n*H), 4.63 (brs, 2*n*H), 7.1-7.4 (brm, 6H), 7.85 (brs, 2H).

Homopolymer **poly-2**: ^{1}H NMR (400MHz, CDCl$_3$) δ 0.88 (brs, 6*n*H), 1.21 (brs, 6*n*H), 1.44

(brs, 2nH), 1.53 (brs, 2nH), 1.59 (brs, 4nH), 2.31 (brs, 6nH), 3.40 (brs, 2nH), 4.53 (brs, 2nH), 4.62 (brs, 2nH), 7.1-7.4 (brm, 6H), 7.85 (brs, 2H).

Random Copolymers **poly-1/(*R*)-2(x/y)** and **poly-1/(*S*)-2(x/y) (x + y = 40)**: ^{1}H NMR (400MHz, $CDCl_3$) δ 0.88 (brs, (6**x**+6**y**)H), 1.21 (brs, 6**y**H), 1.44 (brs, 2**y**H), 1.53 (brs, (4**x**+2**y**)H), 2.30 (brs, (6**x**+6**y**)H), 3.41 (brs, (4**x**+2**y**)H), 4.54 (brs, (2**x**+2**y**)H), 4.62 (brs, (2**x**+2**y**)H), 7.1-7.4 (brm, 6H), 7.85 (brs, 2H).

Homopolymer **poly-3**: ^{1}H NMR (400MHz, $CDCl_3$) δ 0.86 (brs, 12nH), 1.18 (brs, 4nH), 1.26 (brs, 6nH), 1.36 (brs, 6nH), 2.22 (brs, 2nH), 2.61 (brs, 2nH).

Molar ratios of the achiral and chiral monomer units (x:y) can be estimated from the integral ratio of the signals at δ 2.30 (= 240H) and δ 1.21 as shown below. The integral ratio of the two signals (δ 1.21 and δ 2.30) directly reflects the ratio of the two monomers.

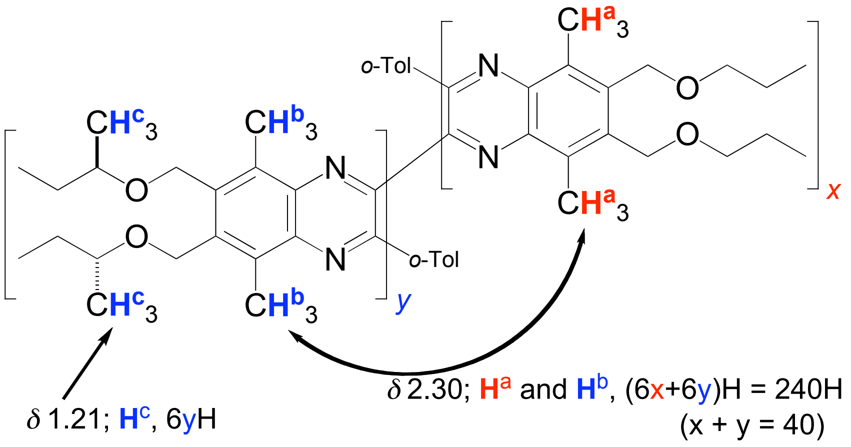

The following graphs demonstrate a linear relationship of the feeding ratio and the NMR integral ratio for **poly-1/(*R*)-2(x/y)** (top) and **poly-1/(*S*)-2(x/y)** (bottom).

Table S3. Ratio of the integral value of δ 2.30 and δ 1.21 in random copolymers using (*R*)-2

content of (*R*)-2	ratio of integral value (H^c/H^a+H^b)
0	0
0.05	0.09
0.1	0.16
0.2	0.25
0.3	0.34
0.5	0.57
0.7	0.72
1	1.08

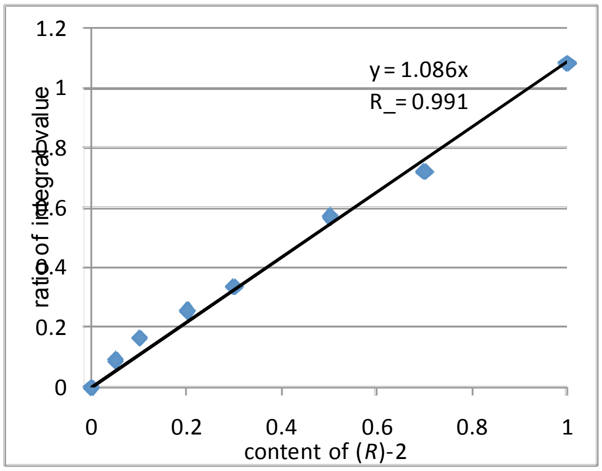

Figure S1. Relationship of the content of (*R*)-**2** and the ratio of the integral value

Table S4. Ratio of the integral value of δ 2.30 and δ 1.21 in random copolymers using (*S*)-2

content of (*S*)-2	ratio of integral value (H^c/H^a+H^b)
0.1	0.15
0.2	0.30
0.3	0.37
0.5	0.55
1	1.02

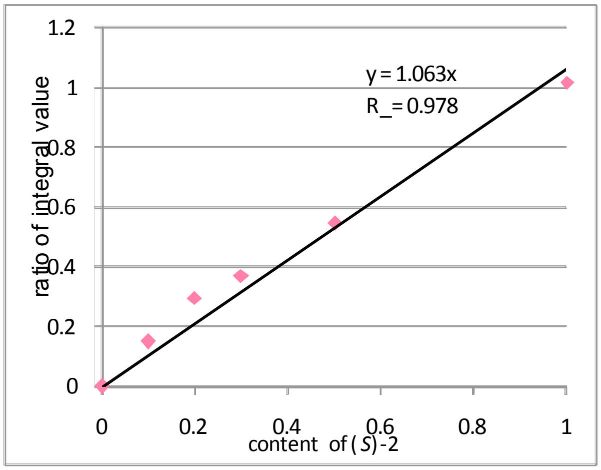

Figure S2. Relationship of the content of (*S*)-**2** and the ratio of the integral value

4. Determination of the screw-sense excess

The screw-sense excesses of the polymers were determined by CD spectra and UV/vis absorption spectra. Here we used the dissymmetry factor g_{abs} ($\Delta\varepsilon/\varepsilon$)[1] to avoid the effects of the concentration errors of the polymer solutions. Firstly, the percent screw-sense excess *se* was defined as

$$se = ([P]-[M]) / ([P]+[M]) \times 100 \qquad (1)$$

where *[P]* and *[M]* are molar concentrations of *P* and *M* helical polymers. In other words, positive *se* means a *P*-enriched state and negative *se* represents *M*-enriched state for practical convenience. The screw-sense excess is directly proportional to g_{abs}: the screw-sense excess could therefore be obtained as a product of g_{abs} and the proportionality factor *F*.

$$se = F \times g_{abs} \qquad (2)$$

On the other hand, the ratio of the molar concentrations of purely M and P helical polymers is given by the Boltzmann distrirution using the energy difference per monomer unit E_h between the *P*- and *M*-helices, the number of chiral unit *N* (40 to -40, positive number means the number of (*R*) monomer units and negative number represents the number of (*S*) monomer units), the gas constant *R* (8.31447 $\mathrm{J{\cdot}K^{-1}{\cdot}mol^{-1}}$), and temperature *T* (298 K) as previously reported.[2]

$$[P]/[M] = \exp(E_h N/RT) \qquad (3)$$

Therefore, the screw-sense excess is expressed as follows.

$$se = \tanh(E_h N/2RT) \qquad (4)$$

Nonlinear least-squares fitting of the screw-sense excess *se* against the number of the chiral unit *N* was performed by using the Solver Function in Microsoft Office Excel 2007. Sums of the squares of the deviation were minimized by varying the proportionality factor *F* and the energy difference per monomer unit E_h. These parameters were successfully converged

---

[1] Fujiki, M. *Macromol. Rapid. Commun.* **2001**, *22*, 539.

[2] Lifson, S.; Andreola, C.; Peterson, N. C.; Green, M. M. *J. Am. Chem. Soc.* **1989**, *111*, 8850.

and the final values were as follows.

$$F = 4.1785\times10^{4}, \quad E_h\ -0.5909\ \mathrm{kJ{\cdot}mol^{-1}} \qquad (5)$$

To evaluate the validity of the obtained value of F, the difference of the energy between P and M helices ΔG, which was obtained from F and g_{abs}, were plotted against the number of chiral unit N. Ideally, ΔG is proportional to the number of chiral unit N, and the gradient represents the energy difference per monomer unit E_h.

$$\Delta G = G^P\text{-}G^M = E_hN = \mathrm{arctanh}(F \times g_{abs})/2RT \qquad (6)$$

The relationships between ΔG and N (12 ~ -12) with varied F (4.1785×10^4 ~ $4.1785\times10^4 \times 0.80$) are shown in Figure S3. Only the region where N is between 12 and -12 is shown, because the values of g_{abs} for $|N| > 12$ are too large to evaluate ΔG accurately. In this region, the effect of the measurement error is not negligible due to the nature of arc hyperbolic tangent function. Goodness of fit, as measured by Pearson R^2, is greater than 0.999 when F is 4.1785×10^4. Smaller F makes the line sigmoidal, and the linearity was not obtained.

Figure S3. The relationships between ΔG and N with varied F.

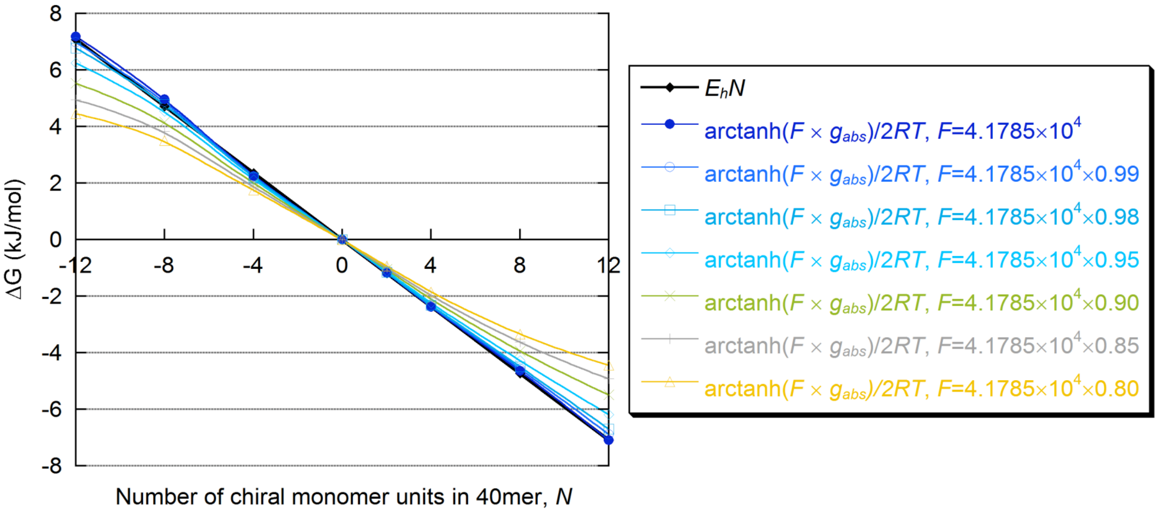

5. CD and UV Spectra of the Polymers

Figure S4. UV/vis absorption spectrum and CD spectrum of **poly-1** in $CHCl_3$ (1.82×10^{-2} g/L).

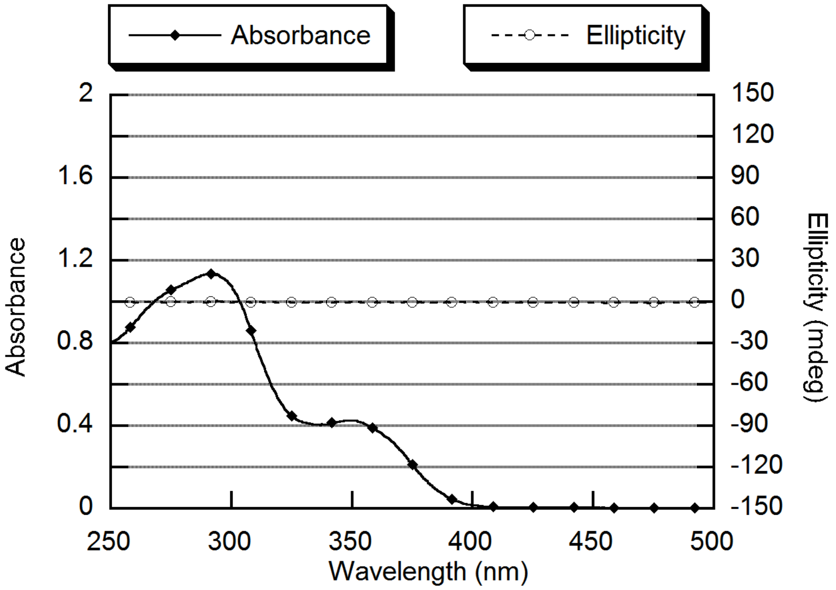

Figure S5. UV/vis absorption spectrum and CD spectrum of **poly-1/(*R*)-2**(38/2) in $CHCl_3$ (2.46×10^{-2} g/L).

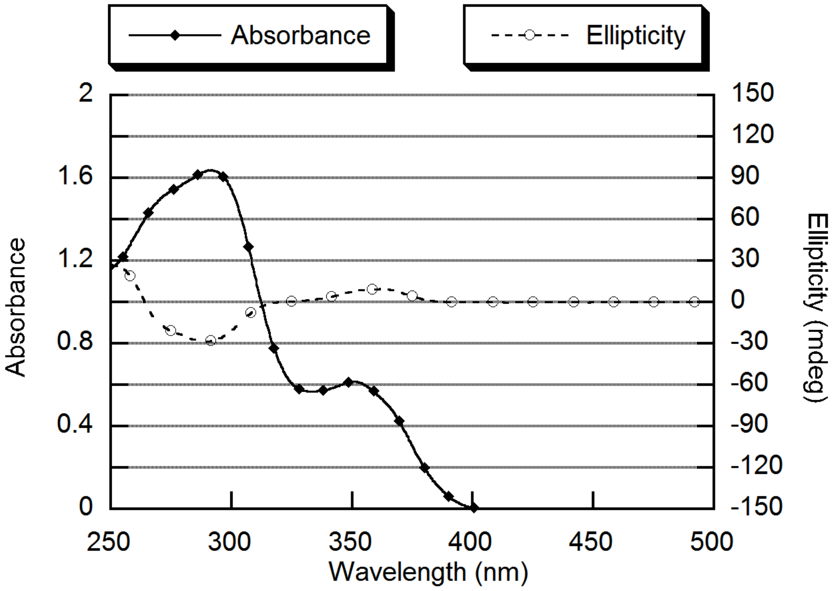

Figure S6. UV/vis absorption spectrum and CD spectrum of **poly-1/(*R*)-2**(36/4) in $CHCl_3$ (1.53×10^{-2} g/L).

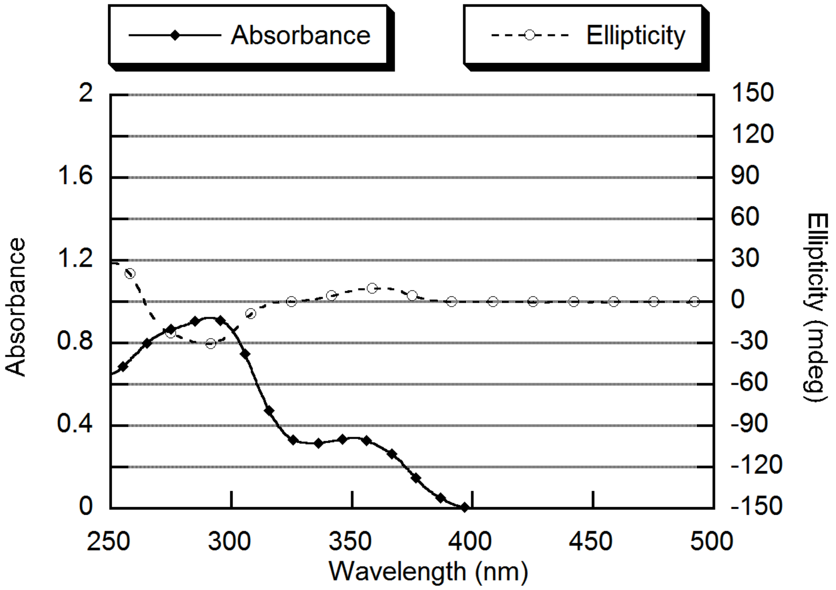

Figure S7. UV/vis absorption spectrum and CD spectrum of **poly-1/(*R*)-2**(32/8) in $CHCl_3$ (1.79×10^{-2} g/L).

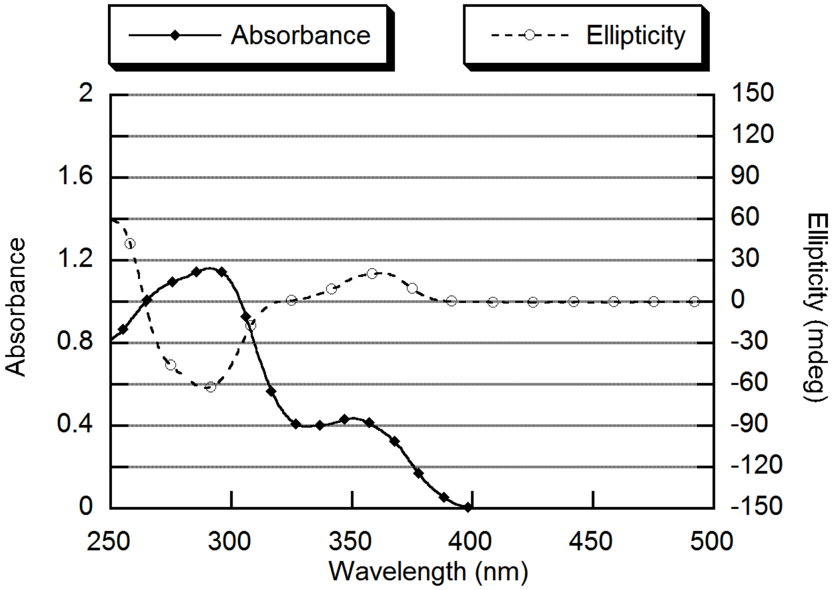

Figure S8. UV/vis absorption spectrum and CD spectrum of **poly-1/(*R*)-2**(28/12) in $CHCl_3$ (1.49×10^{-2} g/L).

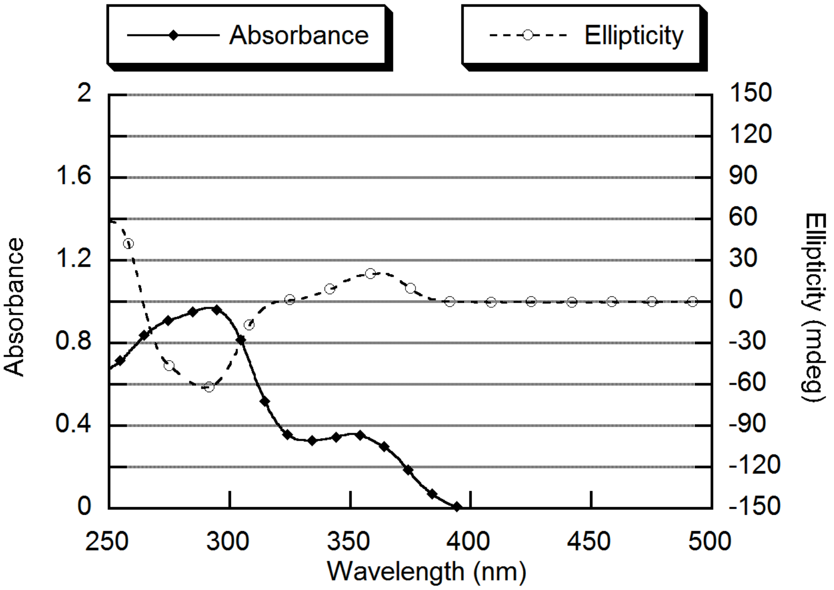

Figure S9. UV/vis absorption spectrum and CD spectrum of **poly-1/(*R*)-2**(20/20) in $CHCl_3$ (2.31×10^{-2} g/L).

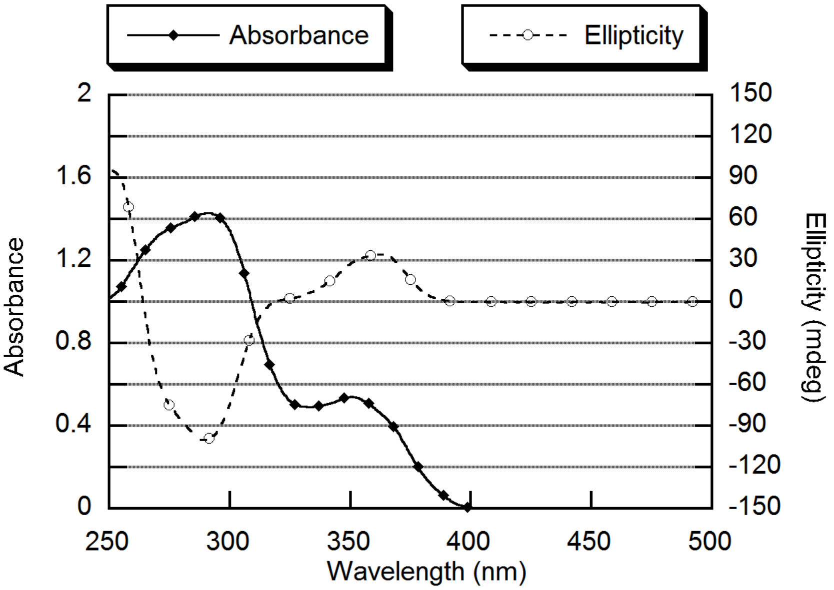

Figure S10. UV/vis absorption spectrum and CD spectrum of **poly-1/(*R*)-2**(12/28) in $CHCl_3$ (2.56×10^{-2} g/L).

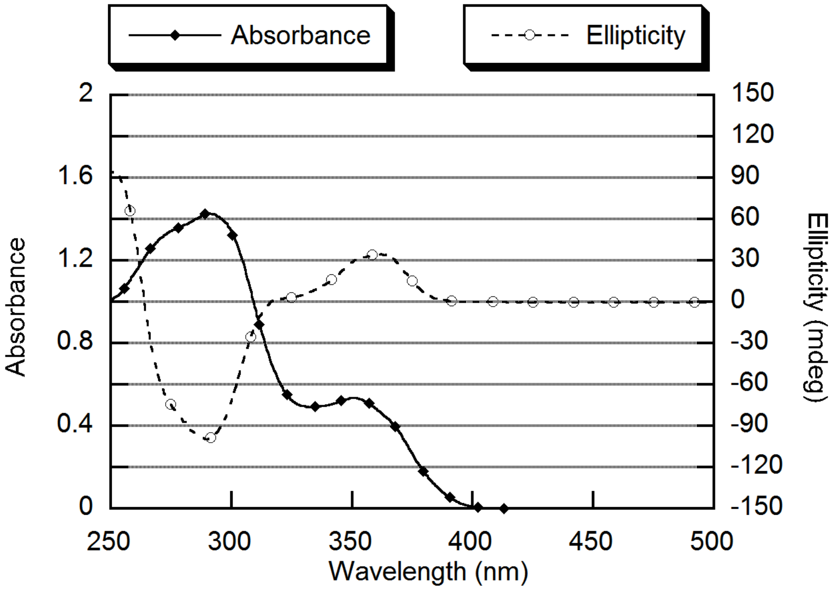

Figure S11. UV/vis absorption spectrum and CD spectrum of **poly-(*R*)-2** in $CHCl_3$ (2.39×10^{-2} g/L).

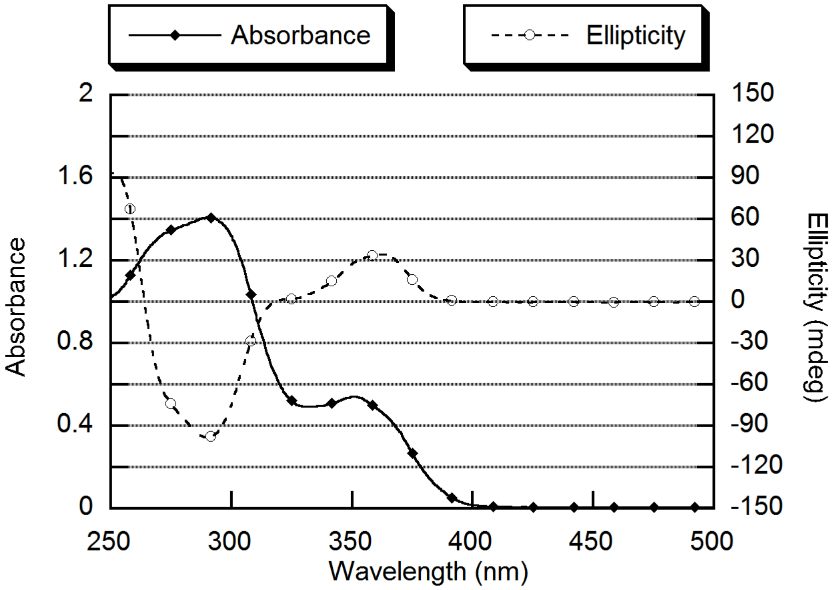

Figure S12. UV/vis absorption spectrum and CD spectrum of **poly-1/(*S*)-2**(36/4) in $CHCl_3$ (2.19×10^{-2} g/L).

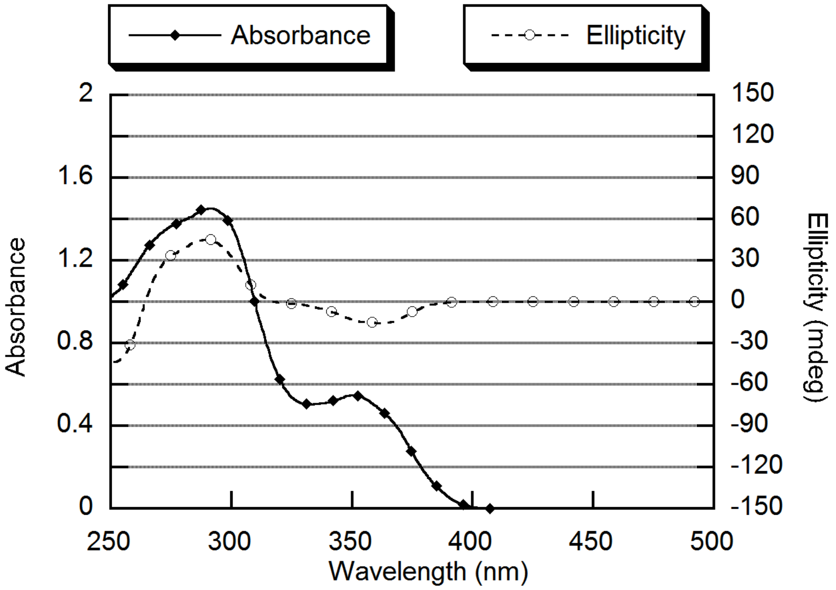

Figure S13. UV/vis absorption spectrum and CD spectrum of **poly-1/(*S*)-2**(32/8) in $CHCl_3$ (1.85×10^{-2} g/L).

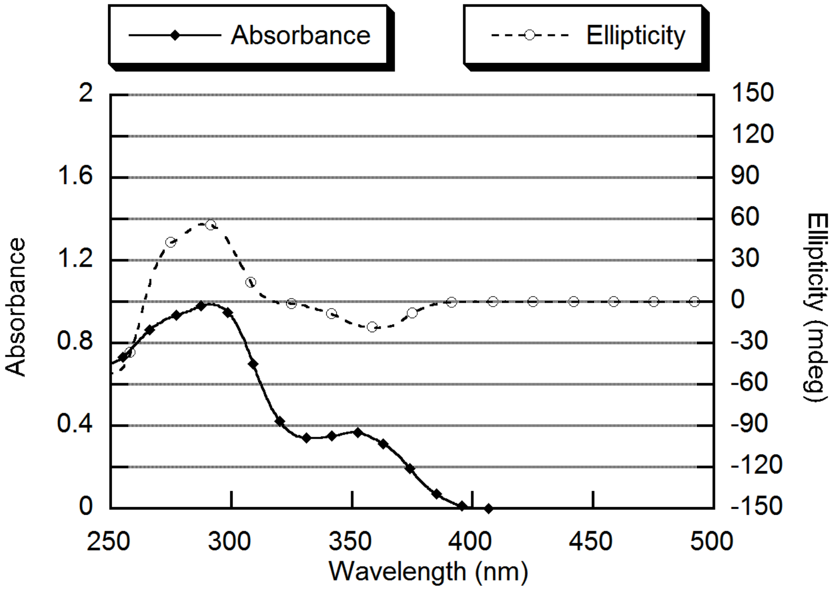

Figure S14. UV/vis absorption spectrum and CD spectrum of **poly-1/(*S*)-2**(28/12) in $CHCl_3$ (2.72×10^{-2} g/L).

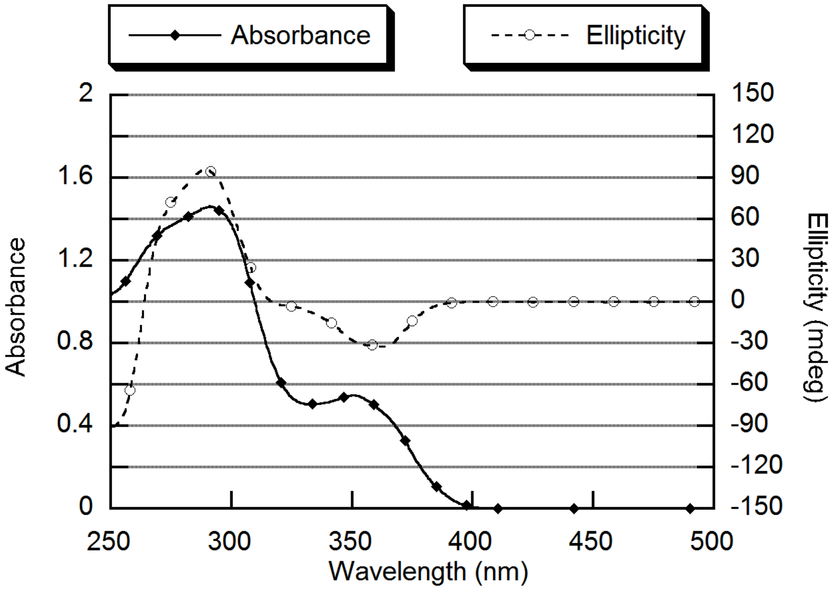

Figure S15. UV/vis absorption spectrum and CD spectrum of **poly-1/(*S*)-2**(20/20) in $CHCl_3$ (2.91×10^{-2} g/L).

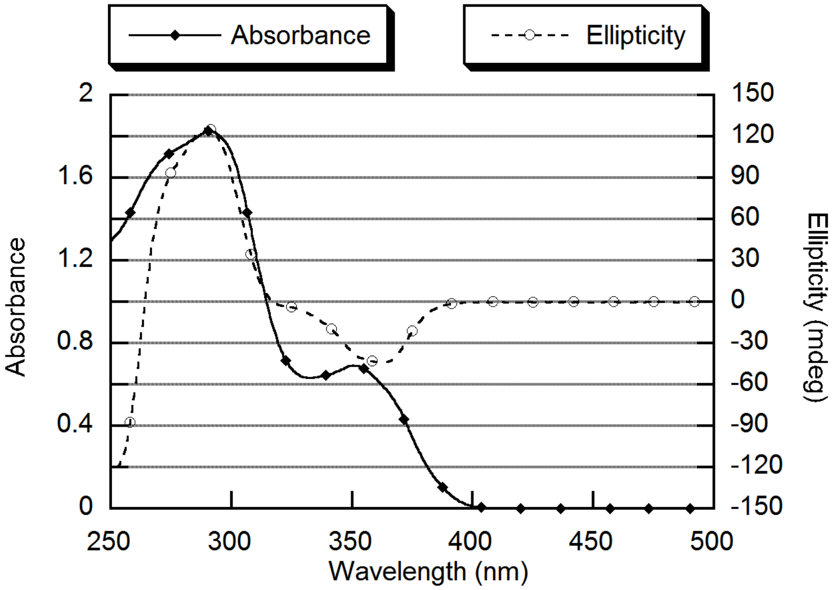

Figure S16. UV/vis absorption spectrum and CD spectrum of **poly-(*S*)-2** in $CHCl_3$ (2.54×10^{-2} g/L).

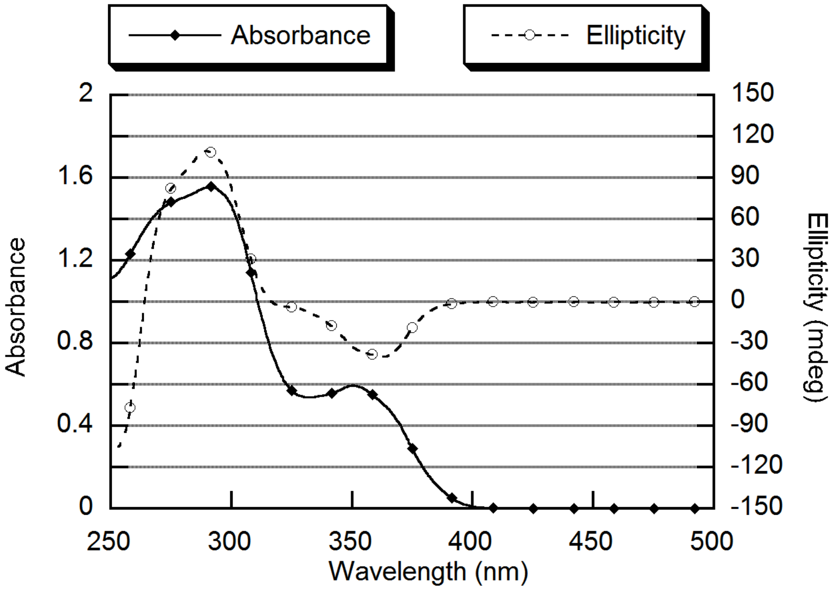

Figure S17. UV/vis absorption spectrum and CD spectrum of **poly-(*R*)-2**(100) in $CHCl_3$ (1.60×10^{-2} g/L).

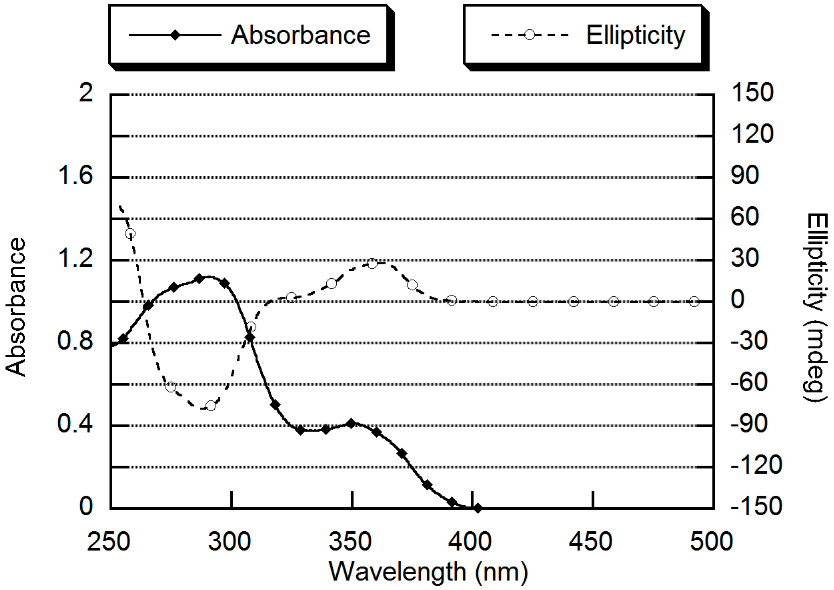

Figure S18. UV/vis absorption spectrum and CD spectrum of **poly-(*R*)-2**(200) in $CHCl_3$ (2.32×10^{-2} g/L).

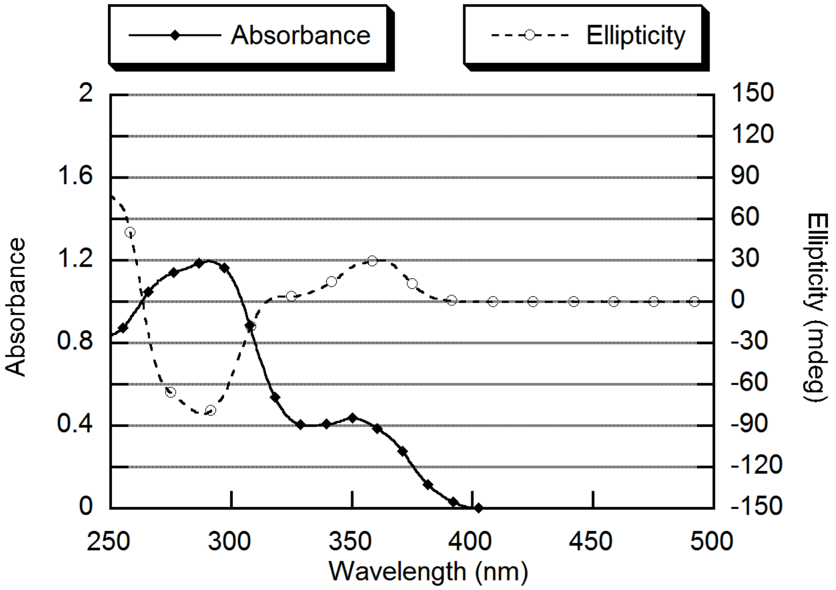

Figure S19. UV/vis absorption spectrum and CD spectrum of **poly-(*R*)-2** in 1,1,2-Trichloroethane/$CHCl_3$ (20:80, v/v, 2.00×10^{-2} g/L).

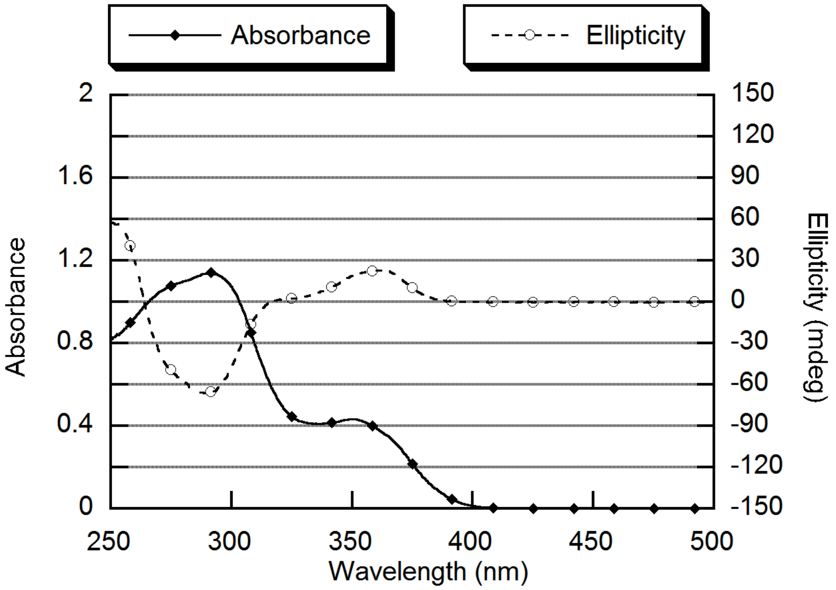

Figure S20. UV/vis absorption spectrum and CD spectrum of **poly-(*R*)-2** in 1,1,2-Trichloroethane/$CHCl_3$ (30:70, v/v, 1.98 × 10^{-2} g/L).

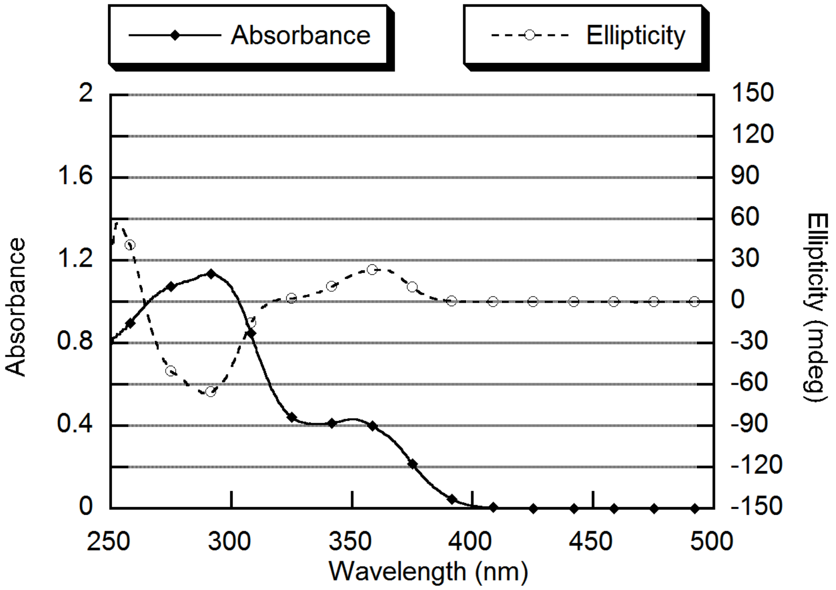

Figure S21. UV/vis absorption spectrum and CD spectrum of **poly-(*R*)-2** in 1,1,2-Trichloroethane/$CHCl_3$ (40:60, v/v, 1.98 × 10^{-2} g/L).

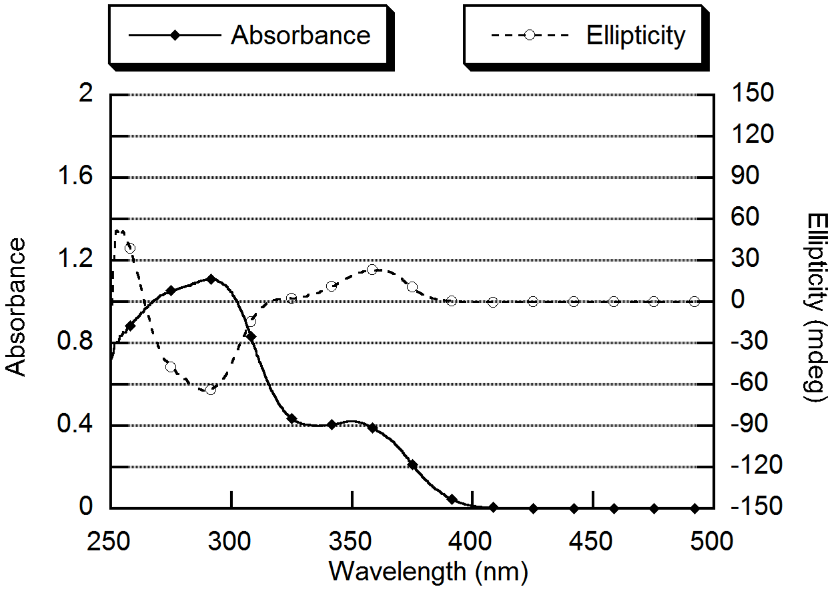

Figure S22. UV/vis absorption spectrum and CD spectrum of **poly-(*R*)-2** in 1,1,2-Trichloroethane/$CHCl_3$ (50:50, v/v, 1.45 × 10^{-2} g/L).

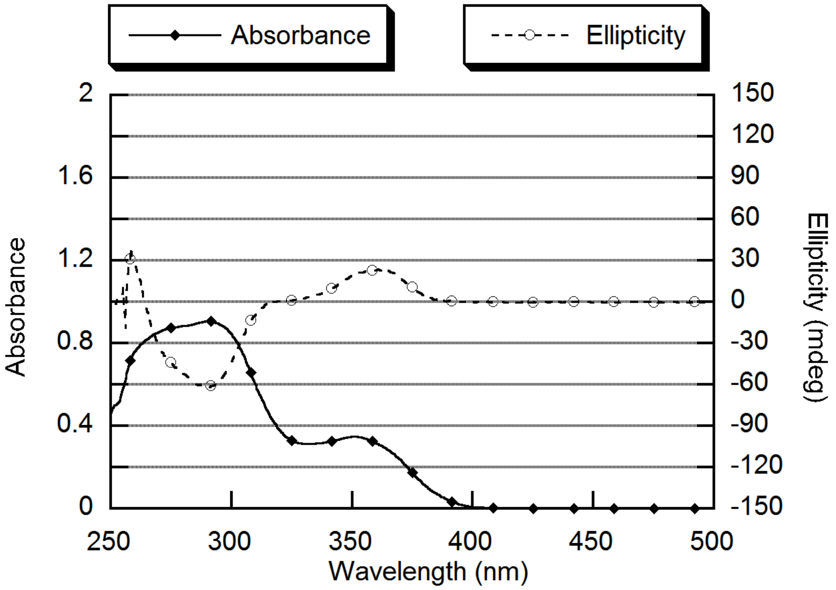

Figure S23. UV/vis absorption spectrum and CD spectrum of **poly-(*R*)-2** in 1,1,2-Trichloroethane/$CHCl_3$ (55:45, v/v, 1.45 × 10^{-2} g/L).

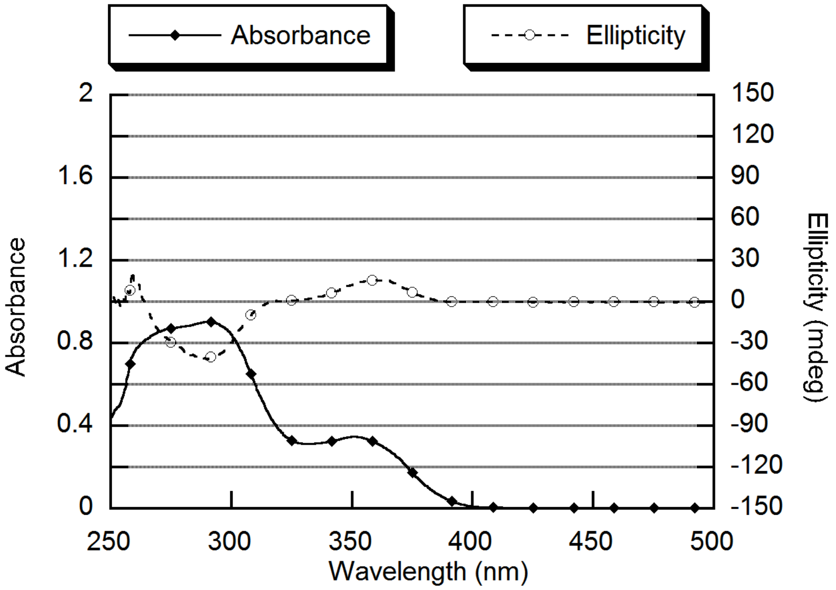

Figure S24. UV/vis absorption spectrum and CD spectrum of **poly-(*R*)-2** in 1,1,2-Trichloroethane/$CHCl_3$ (60:40, v/v, 1.45 × 10^{-2} g/L).

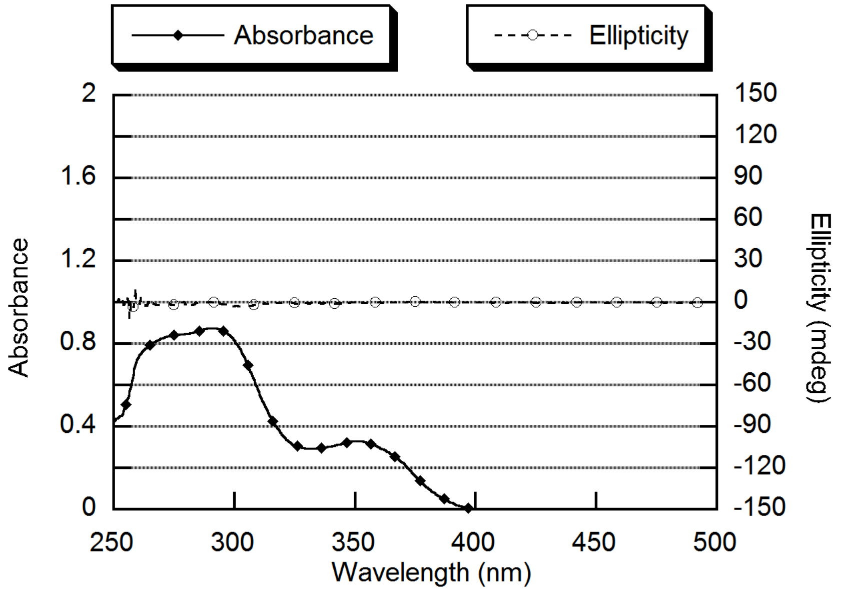

Figure S25. UV/vis absorption spectrum and CD spectrum of **poly-(*R*)-2** in 1,1,2-Trichloroethane/$CHCl_3$ (70:30, v/v, 1.98 × 10^{-2} g/L).

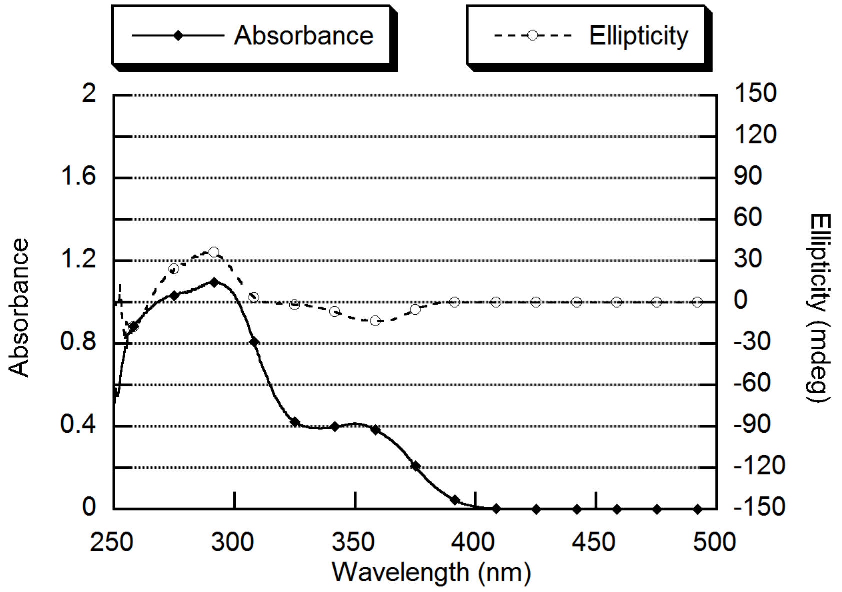

Figure S26. UV/vis absorption spectrum and CD spectrum of **poly-(*R*)-2** in 1,1,2-Trichloroethane/$CHCl_3$ (80:20, v/v, 1.98 × 10^{-2} g/L).

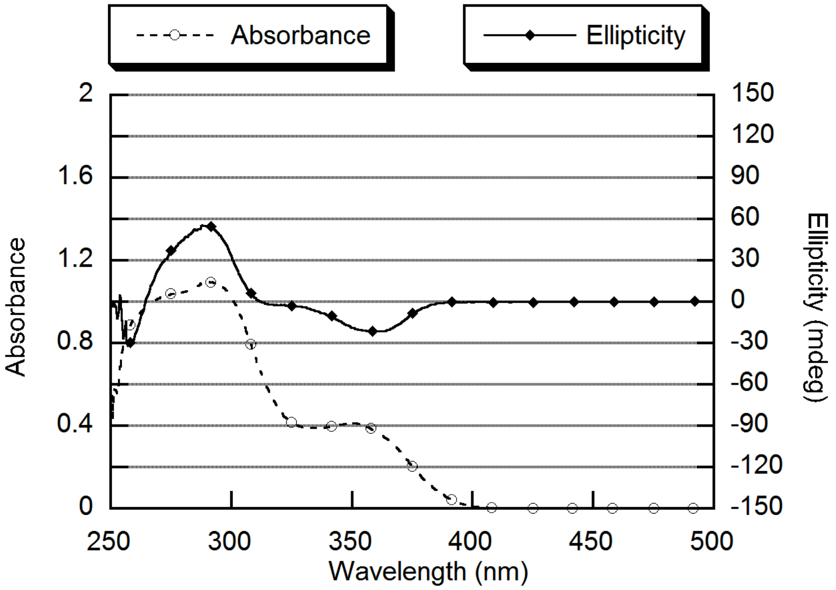

Figure S27. UV/vis absorption spectrum and CD spectrum of **poly-(*R*)-2** in 1,1,2-Trichloroethane/$CHCl_3$ (90:10, v/v, 1.98 × 10^{-2} g/L).

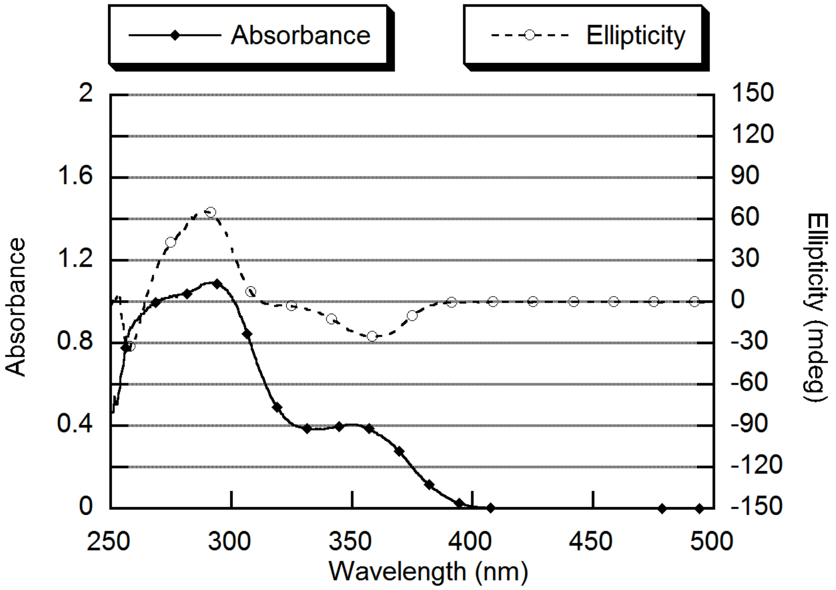

Figure S28. UV/vis absorption spectrum and CD spectrum of **poly-(*R*)-2** in 1,1,2-Trichloroethane (2.01 × 10^{-2} g/L).

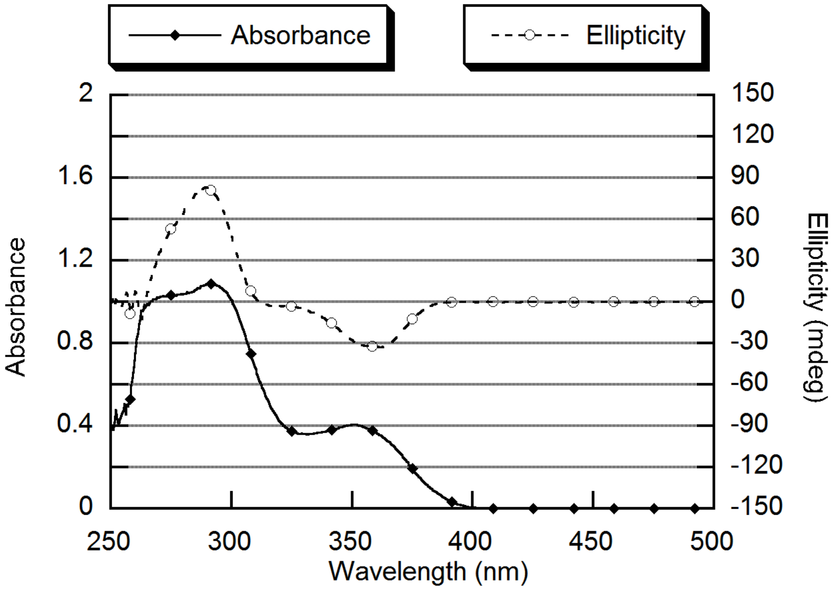

Figure S29. UV/vis absorption spectrum and CD spectrum of **poly-1/(*R*)-2**(12/28) in 1,1,2-Trichloroethane (1.47 × 10^{-2} g/L).

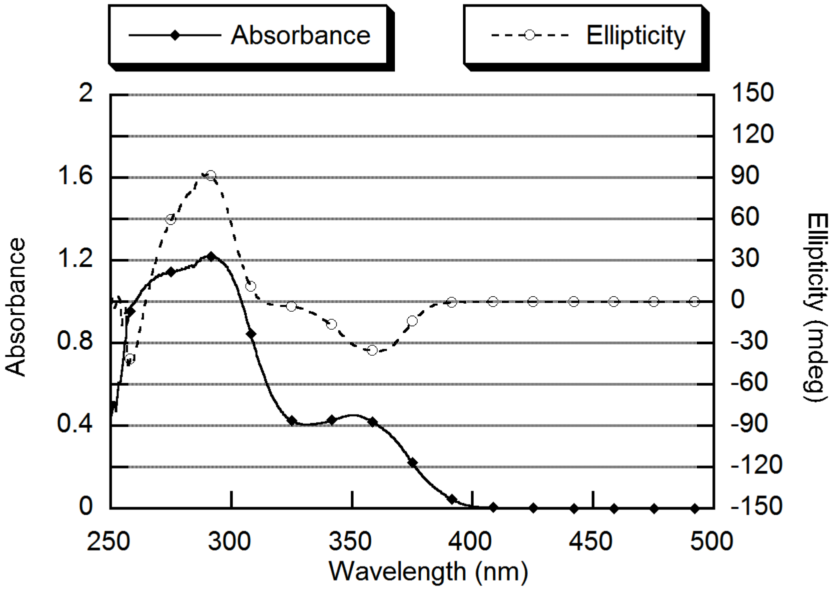

Figure S30. UV/vis absorption spectrum and CD spectrum of **poly-1/(*R*)-2**(20/20) in 1,1,2-Trichloroethane (2.32 × 10^{-2} g/L).

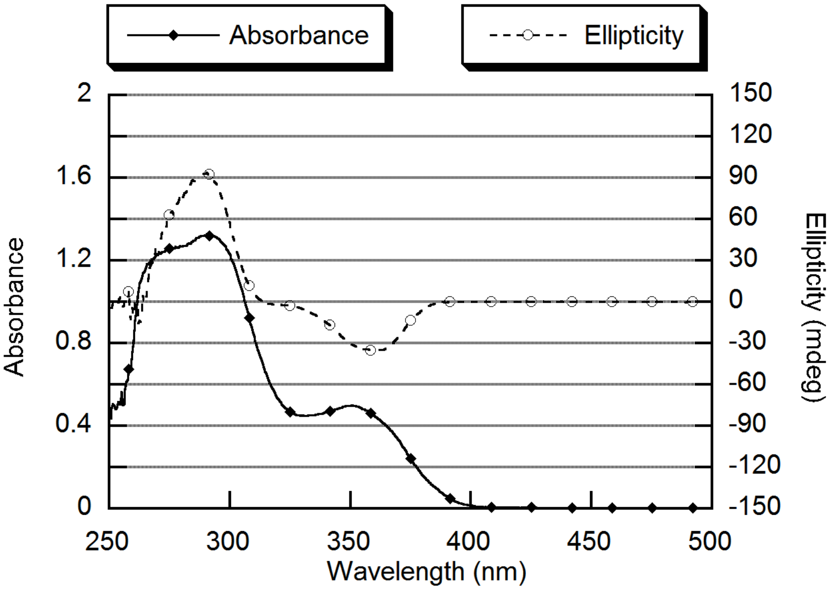

Figure S31. UV/vis absorption spectrum and CD spectrum of **poly-1/(*R*)-2**(28/12) in 1,1,2-Trichloroethane (1.84 × 10^{-2} g/L).

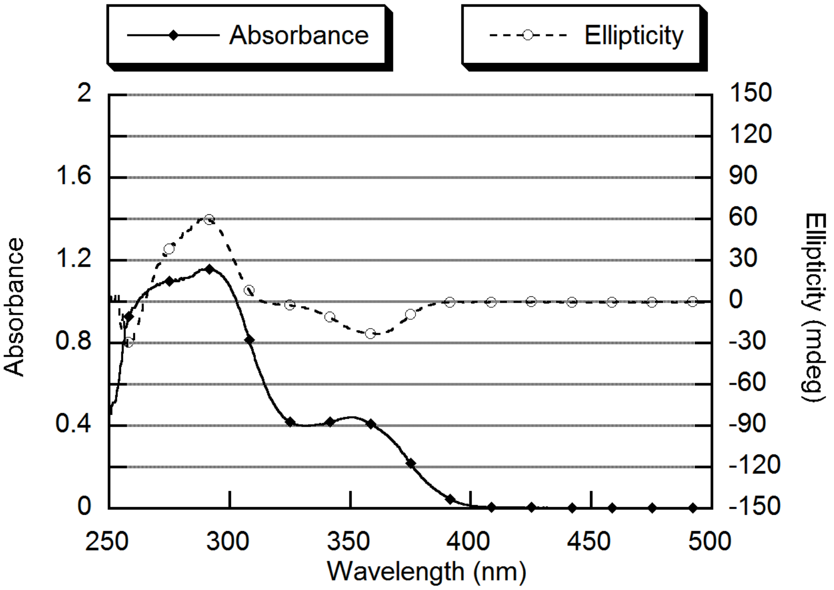

Figure S32. UV/vis absorption spectrum and CD spectrum of **poly-1/(*R*)-2**(32/8) in 1,1,2-Trichloroethane (2.17 × 10^{-2} g/L).

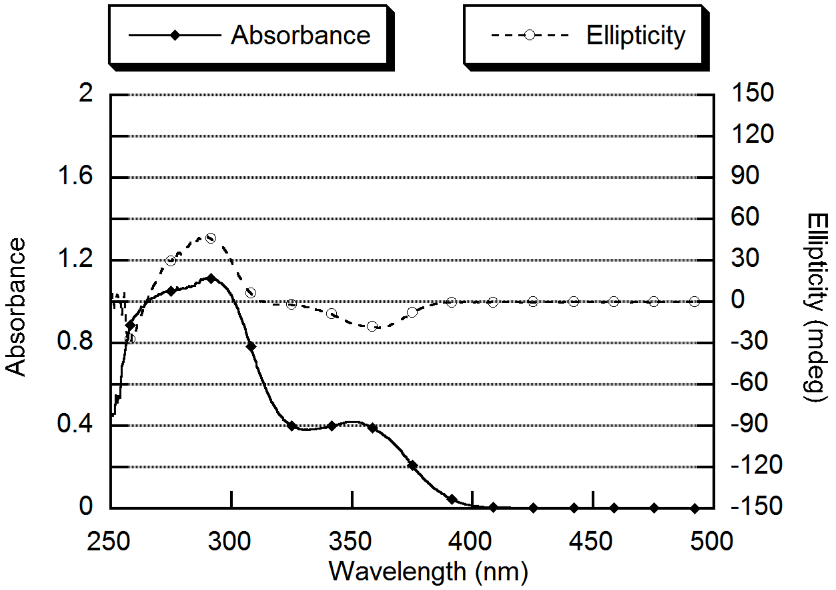

Figure S33. UV/vis absorption spectrum and CD spectrum of **poly-1/(*R*)-2**(36/4) in 1,1,2-Trichloroethane (1.60 × 10^{-2} g/L).

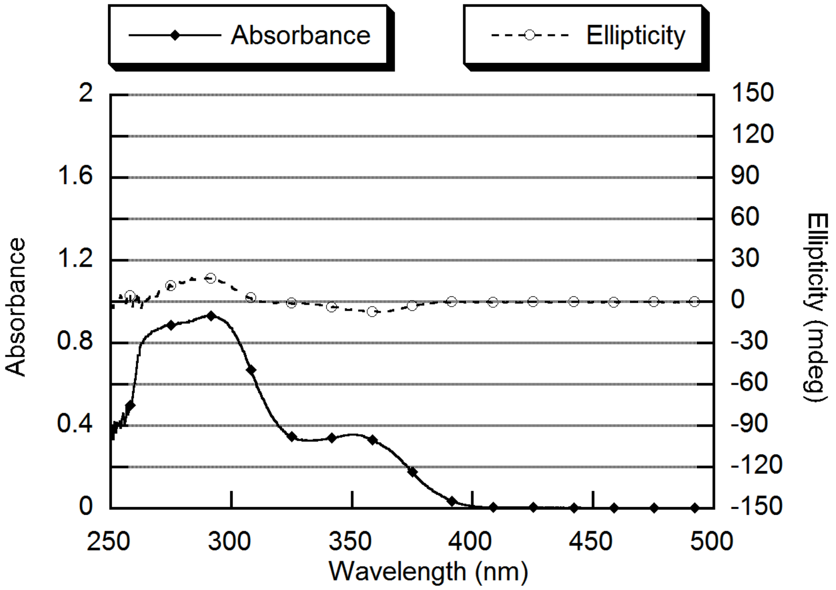

Figure S34. UV/vis absorption spectrum and CD spectrum of **poly-1/(*R*)-2**(38/2) in 1,1,2-Trichloroethane (1.31 × 10^{-2} g/L).

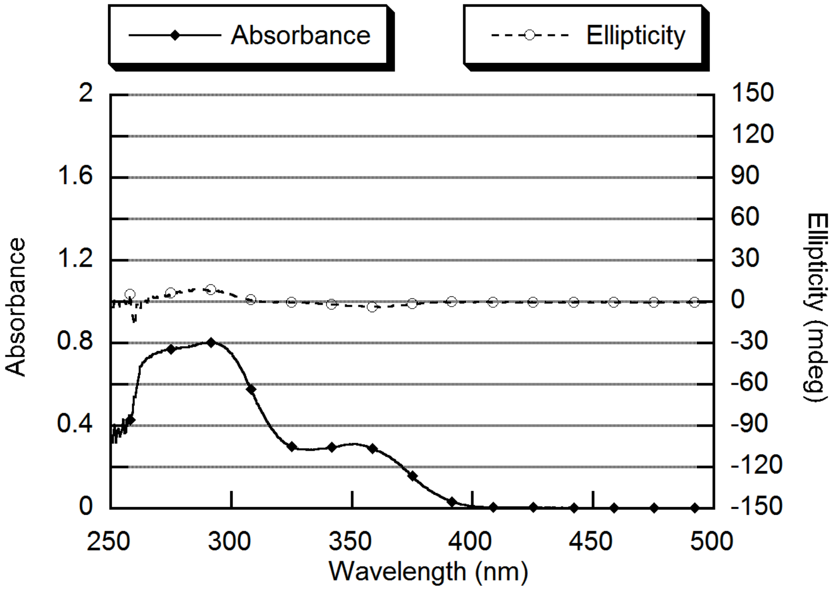

Figure S35. UV/vis absorption spectrum and CD spectrum of **poly-1** in 1,1,2-Trichloroethane (1.82 × 10^{-2} g/L).

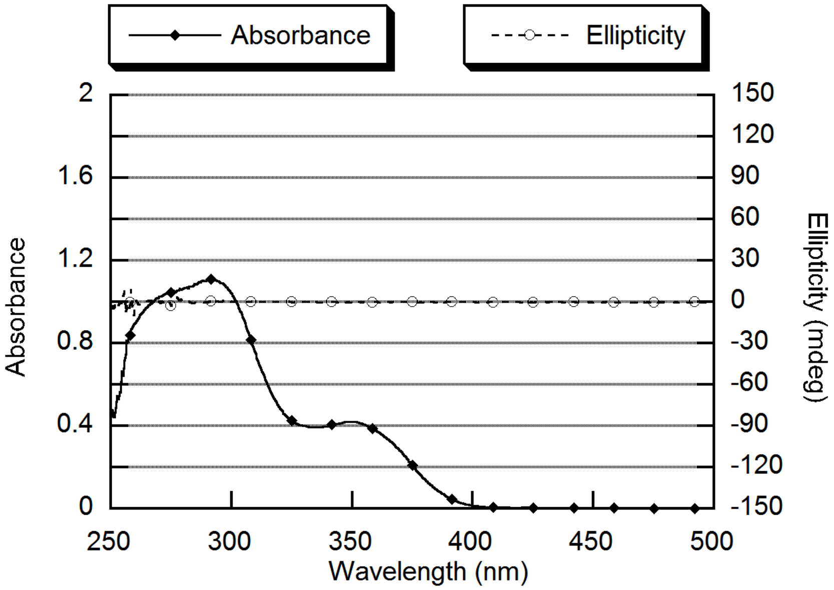

Figure S36. UV/vis absorption spectrum and CD spectrum of **poly-1/(*S*)-2**(36/4) in 1,1,2-Trichloroethane (1.86 × 10^{-2} g/L).

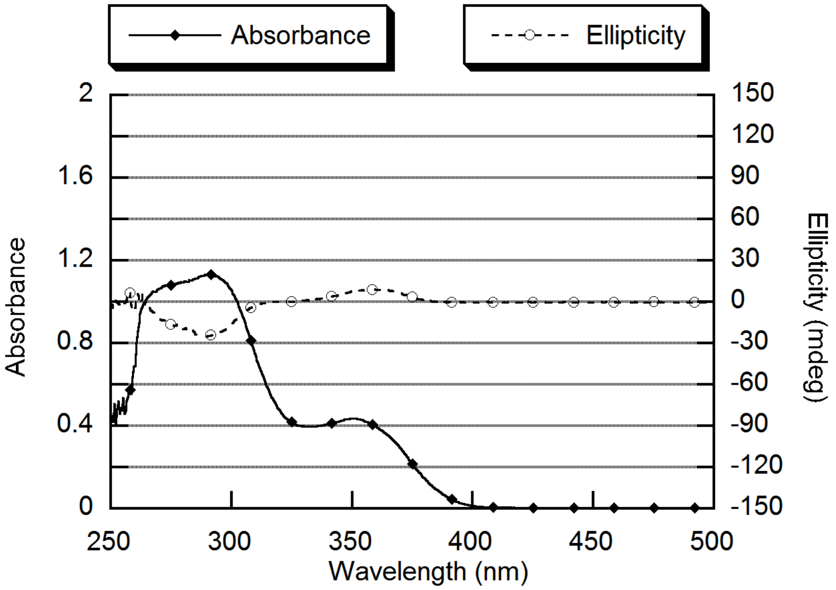

Figure S37. UV/vis absorption spectrum and CD spectrum of **poly-1/(*S*)-2**(32/8) in 1,1,2-Trichloroethane (2.10× 10^{-2} g/L).

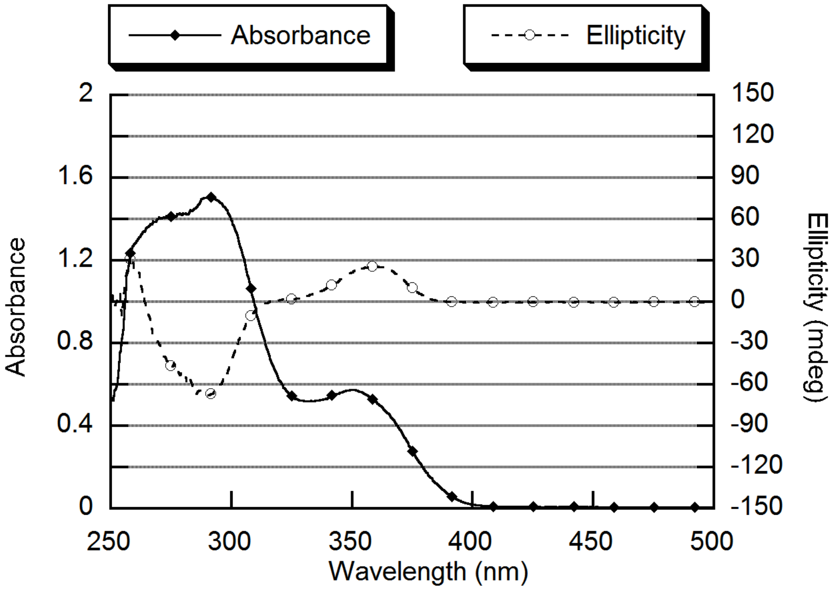

Figure S38. UV/vis absorption spectrum and CD spectrum of **poly-1/(*S*)-2**(28/12) in 1,1,2-Trichloroethane (2.36 × 10^{-2} g/L).

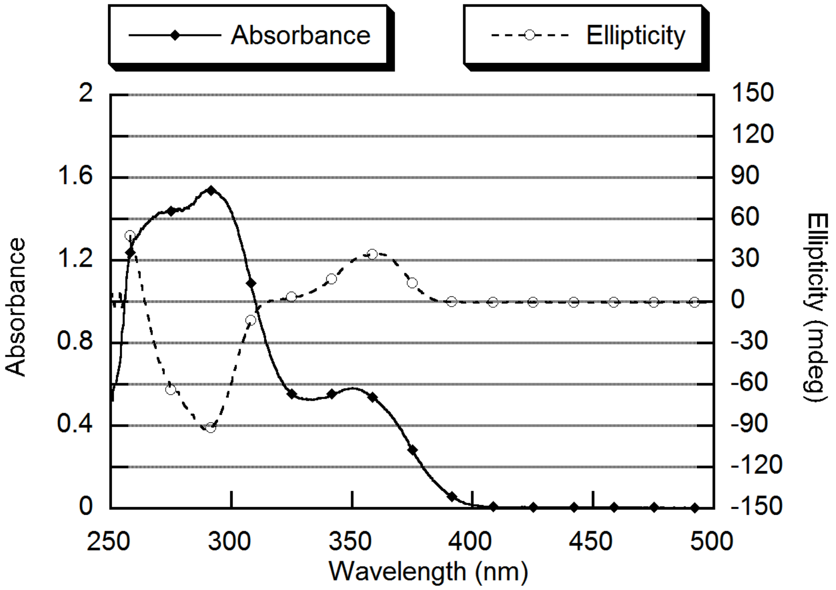

Figure S39. UV/vis absorption spectrum and CD spectrum of **poly-1/(*S*)-2**(20/20) in 1,1,2-Trichloroethane (1.34 × 10^{-2} g/L).

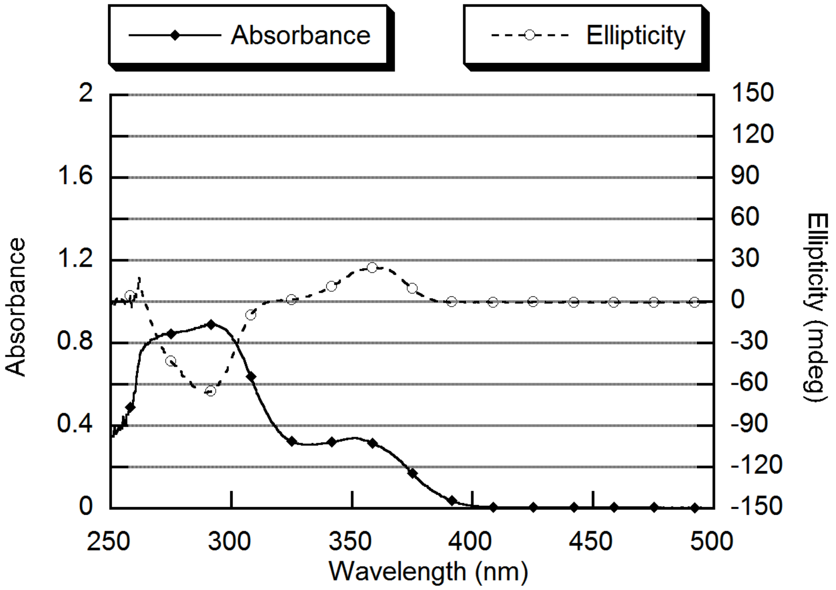

Figure S40. UV/vis absorption spectrum and CD spectrum of **poly-(*S*)-2** in 1,1,2-Trichloroethane (1.86×10^{-2} g/L).

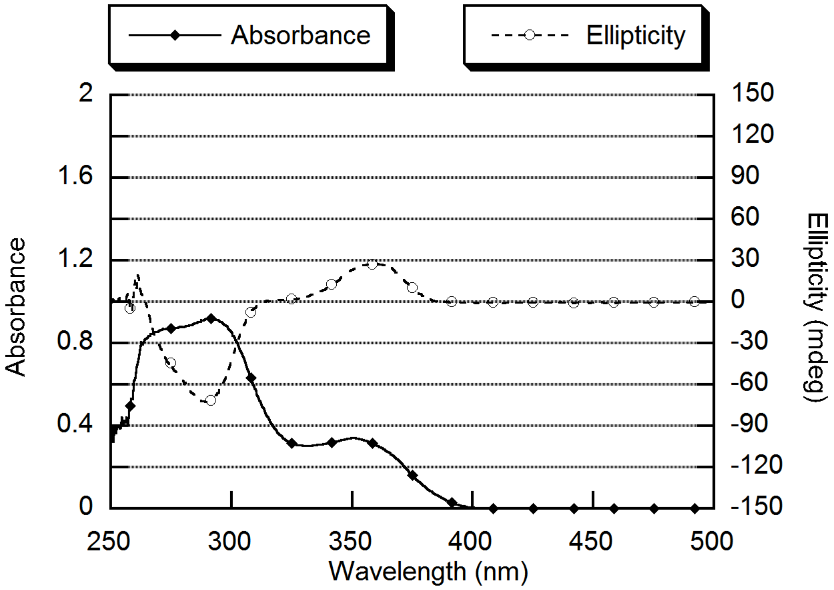

Figure S41. UV/vis absorption spectrum and CD spectrum of **poly-(*R*)-2** in dichloromethane (1.95×10^{-2} g/L).

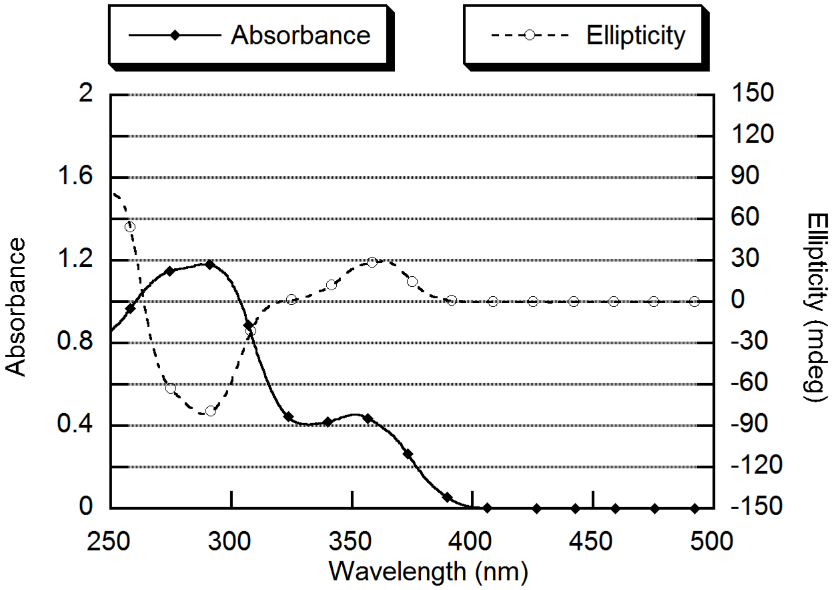

Figure S42 UV/vis absorption spectrum and CD spectrum of **poly-(*R*)-2** in tetrahydrofuran (2.41 × 10^{-2} g/L).

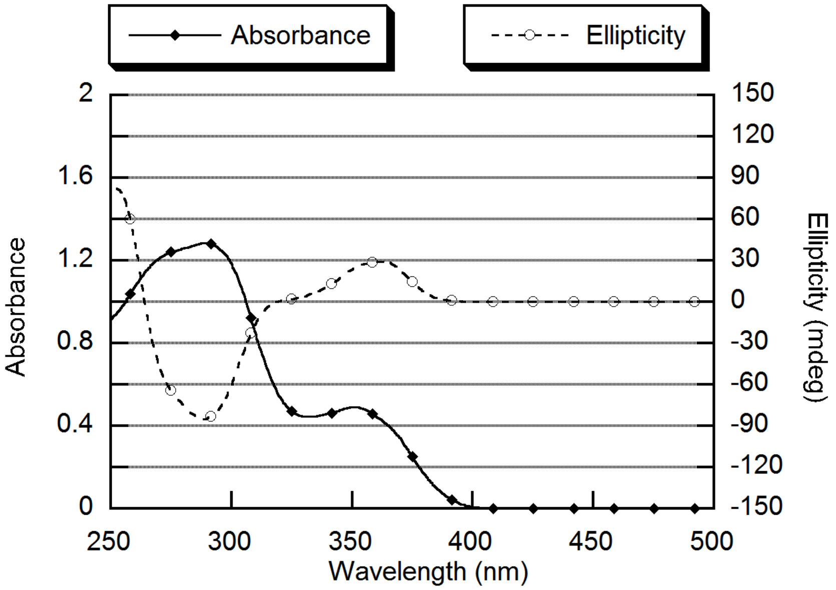

Figure S43. UV/vis absorption spectrum and CD spectrum of **poly-(*R*)-2** in 1-butanol (1.66 × 10^{-2} g/L).

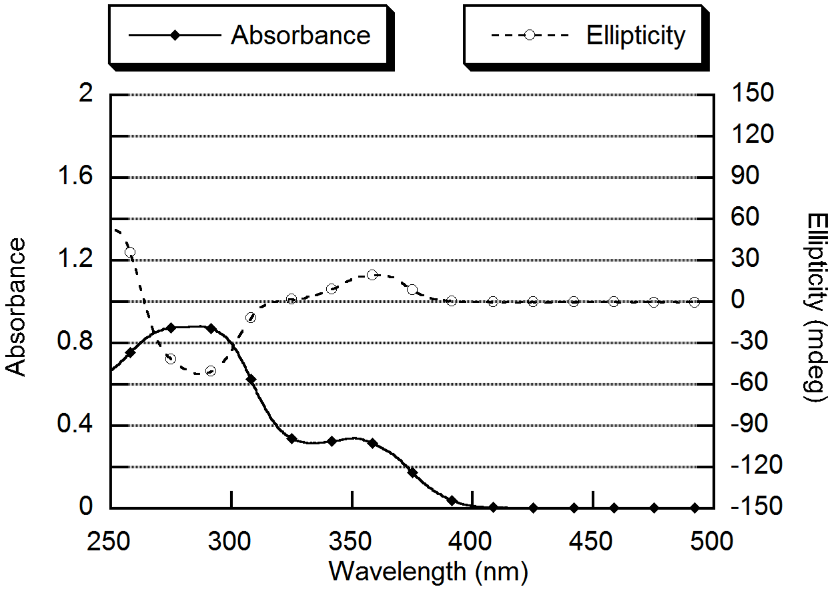

Figure S44. UV/vis absorption spectrum and CD spectrum of **poly-(*R*)-2** in 1,1,1-trichloroethane (1.40 × 10^{-2} g/L).

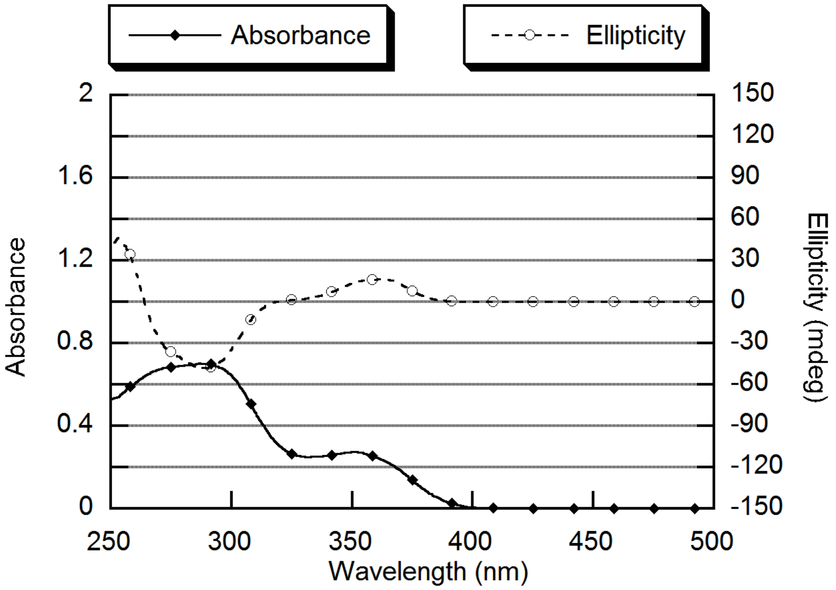

Figure S45. UV/vis absorption spectrum and CD spectrum of **poly-(*R*)-2** in 1-chlorobutane (1.73 × 10^{-2} g/L).

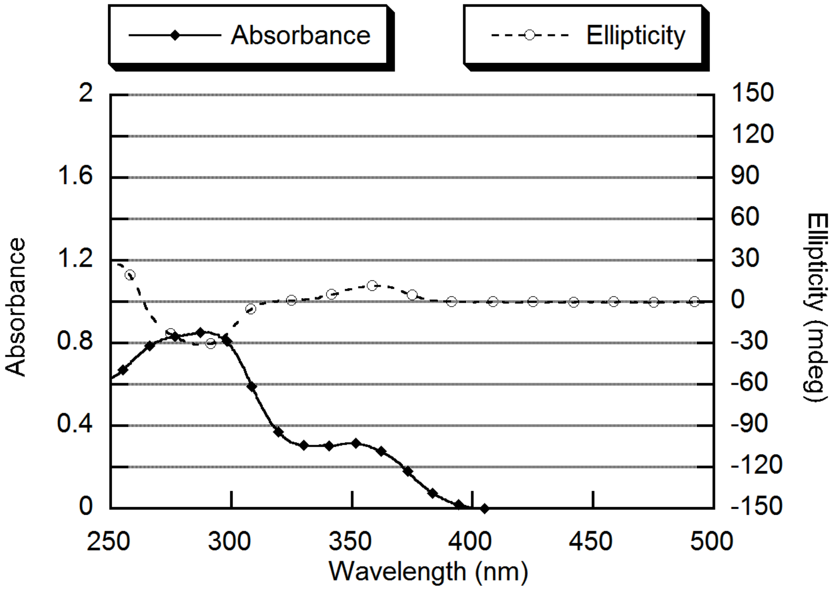

Figure S46. UV/vis absorption spectrum and CD spectrum of **poly-(*R*)-2**(100) in 1-chlorobutane (1.73×10^{-2} g/L).

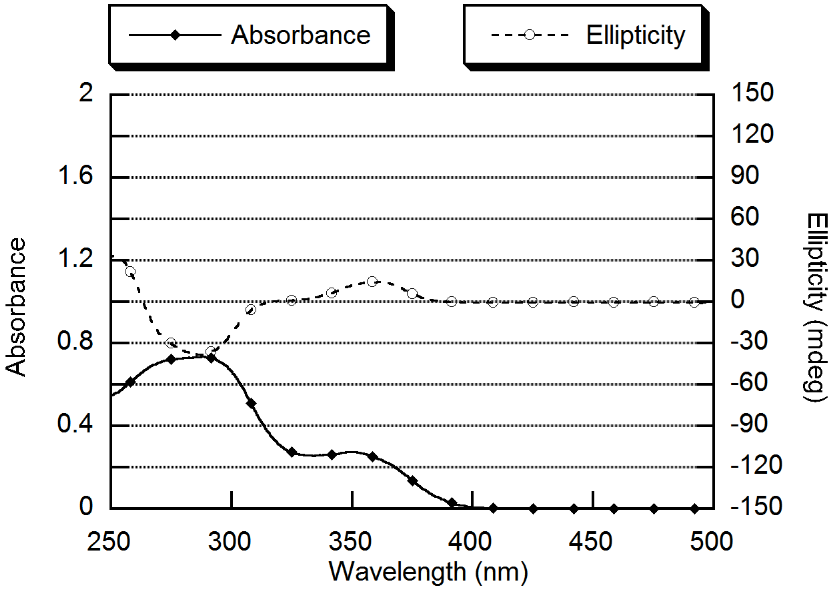

Figure S47. UV/vis absorption spectrum and CD spectrum of **poly-(*R*)-2**(200) in 1-chlorobutane (0.99×10^{-2} g/L).

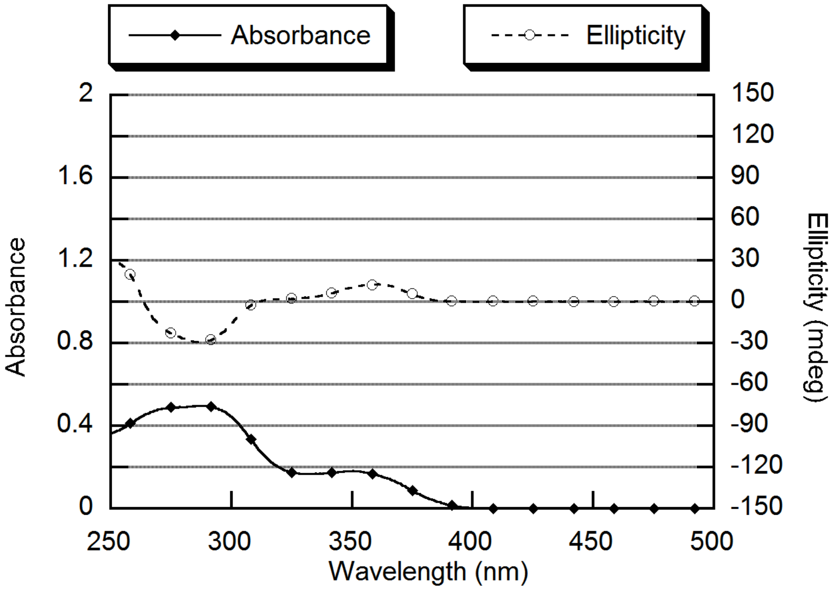

Figure S48. UV/vis absorption spectrum and CD spectrum of **poly-(*R*)-2** in 1-bromobutane (1.77×10^{-2} g/L).

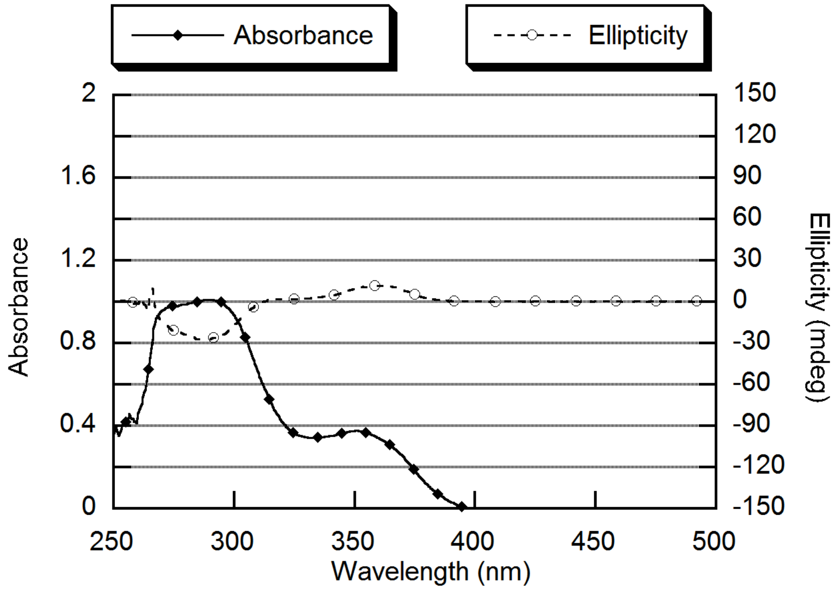

Figure S49. UV/vis absorption spectrum and CD spectrum of **poly-(*R*)-2** in valeronitrile (2.10×10^{-2} g/L).

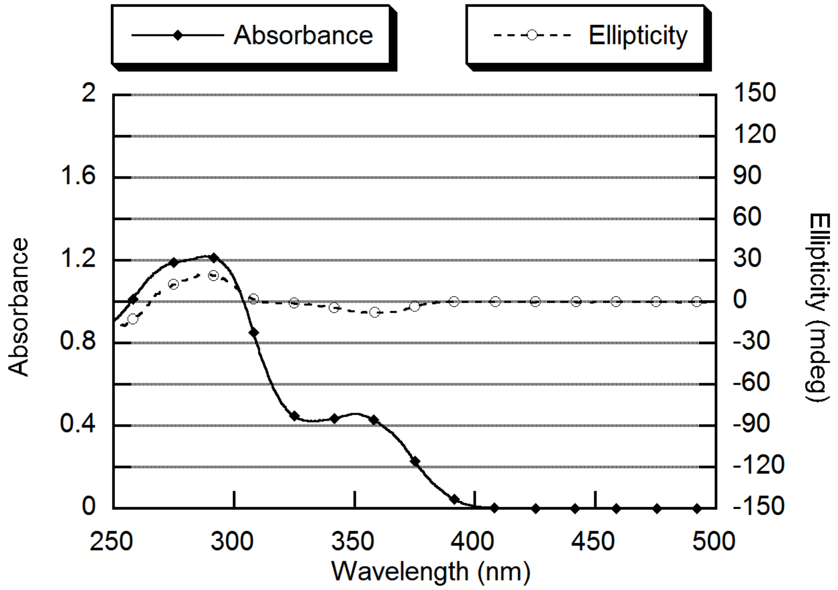

Figure S50. UV/vis absorption spectrum and CD spectrum of **poly-(*R*)-2** in 1,2-dichloroetane (2.33 × 10^{-2} g/L).

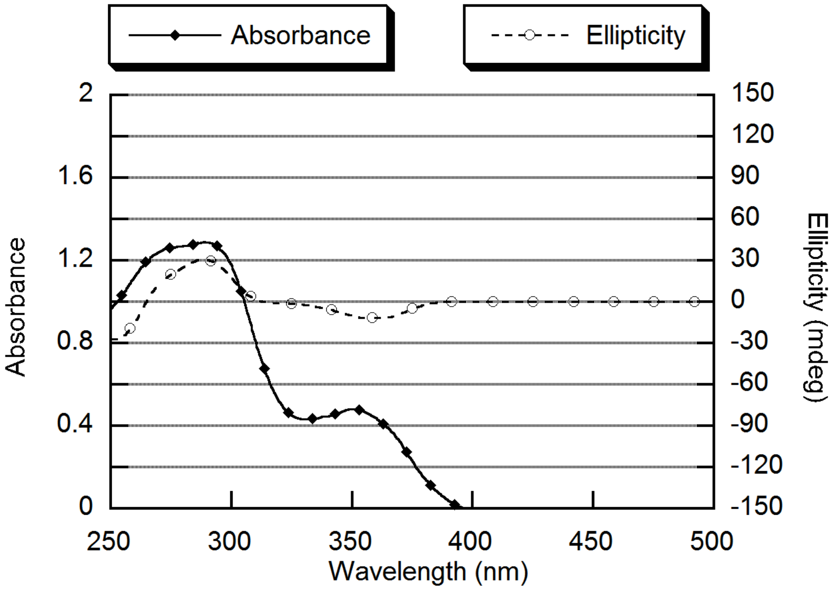

Figure S51. UV/vis absorption spectrum and CD spectrum of **poly-(*R*)-2** in 1,3-dichloropropane (1.81 × 10^{-2} g/L).